The Plant Cell, Vol. 17, 1073–1089, April 2005, www.plantcell.org

Ubiquitous and Endoplasmic Reticulum–Located Lysophosphatidyl Acyltransferase, LPAT2, Is Essential for Female but Not Male Gametophyte Development in Arabidopsis

Hyun Uk Kim,[1] Yubing Li, and Anthony H.C. Huang[2]

Department of Botany and Plant Sciences, Center for Plant Cell Biology, University of California, Riverside, California 92521

Lysophosphatidyl acyltransferase (LPAT) is a pivotal enzyme controlling the metabolic flow of lysophosphatidic acid into different phosphatidic acids in diverse tissues. We examined putative *LPAT* genes in *Arabidopsis thaliana* and characterized two related genes that encode the cytoplasmic LPAT. *LPAT*2 is the lone gene that encodes the ubiquitous and endoplasmic reticulum (ER)–located LPAT. It could functionally complement a bacterial mutant with defective LPAT. LPAT2 and 3 synthesized in recombinant bacteria and yeast possessed in vitro enzyme activity higher on 18:1-CoA than on 16:0-CoA. *LPAT*2 was expressed ubiquitously in diverse tissues as revealed by RT-PCR, profiling with massively parallel signature sequencing, and promoter-driven β-glucuronidase gene expression. LPAT2 was colocalized with calreticulin in the ER by immunofluorescence microscopy and subcellular fractionation. *LPAT*3 was expressed predominately but more actively than *LPAT*2 in pollen. A null allele (*lpat*2) having a T-DNA inserted into *LPAT*2 was identified. The heterozygous mutant (*LPAT*2/*lpat*2) had minimal altered vegetative phenotype but produced shorter siliques that contained normal seeds and remnants of aborted ovules in a 1:1 ratio. Results from selfing and crossing it with the wild type revealed that *lpat*2 caused lethality in the female gametophyte but not the male gametophyte, which had the redundant LPAT3. *LPAT*2-cDNA driven by an *LPAT*2 promoter functionally complemented *lpat*2 in transformed heterozygous mutants to produce the *lpat*2/*lpat*2 genotype. *LPAT*3-cDNA driven by the *LPAT*2 promoter could rescue the *lpat*2 female gametophytes to allow fertilization to occur but not to full embryo maturation. Two other related genes, putative *LPAT*4 and 5, were expressed ubiquitously albeit at low levels in diverse organs. When they were expressed in bacteria or yeast, the microbial extract did not contain LPAT activity higher than the endogenous LPAT activity. Whether *LPAT*4 and 5 encode LPATs remains to be elucidated.

INTRODUCTION

In seed plants, glycerolipids are the most abundant lipids (Somerville et al., 2000; Voelker and Kinney, 2001). They are present as polar lipids in membranes and neutral lipids in storage organs and as biological mediators. They are synthesized via two similar pathways but in distinct subcellular compartments. The two pathways are described as the prokaryotic and eukaryotic systems on the basis of their evolutionary origins. In the prokaryotic system of the plastids, glycerol-3-phosphate (GP) is acylated sequentially with acyl-acyl carrier protein (ACP) to lysophosphatidic acid (LPA) and phosphatidic acid (PA), which are catalyzed by GP acyltransferase (GPAT; EC 2.3.1.15) and LPA acyltransferase (LPAT; EC 2.3.1.51), respectively. PA is converted to different glycolipids and sulfolipids for membrane synthesis within the plastids. In the eukaryotic system of mainly the endoplasmic reticulum (ER), GP is acylated sequentially with acyl-CoA to LPA and PA, which are also catalyzed by GPAT and LPAT, respectively. PA is converted to phospholipids for incorporation into the ER membranes, which will eventually be distributed throughout the cell to become membranes of different cytoplasmic cell components. Some of the cytoplasm-synthesized glycerolipids could be channeled to the plastids to be converted to glycolipids and sulfolipids. In maturing seeds, the cytoplasm-synthesized PA is also converted to triacylglycerols (TAGs) for storage. The prokaryotic and eukaryotic glycerolipid syntheses are similar in the two-enzymic conversion of GP to PA and different in the subsequent diversion of PA to special structural, storage, and signal lipids. The regulation of PA synthesis before the diversion is thus important in the early metabolic control of glycerolipid synthesis. Although the two-enzymic acylations of the prokaryotic and eukaryotic systems are similar, they are catalyzed by enzymes unique to the respective system.

The plastid GPAT in general has an in vitro substrate preference for 18:1-ACP, and in some chilling-sensitive plants, it can use both 18:1- and 16:0-ACP. Its encoded genes in several plant species have been studied (Ishizaki et al., 1988;

[1] Current address: Institute of Biological Chemistry, Washington State University, Pullman, WA 99164-6340.

[2] To whom correspondence should be addressed. E-mail anthony.huang@ucr.edu; fax 951-827-4437.

The author responsible for distribution of materials integral to the findings presented in this article in accordance with the policy described in the Instructions for Authors (www.plantcell.org) is: Anthony H.C. Huang (anthony.huang@ucr.edu).

Article, publication date, and citation information can be found at www.plantcell.org/cgi/doi/10.1105/tpc.104.030403.

Murata and Tasaka, 1997). In *Arabidopsis thaliana*, only one gene, At*GPAT* (*ATS*1), encodes the plastid GPAT. A homozygous mutant defective in this gene has minimal prokaryotic GPAT activity but no major altered phenotype (Kunst et al., 1988). Analysis of the lipid compositions of the homozygous mutant has led to the suggestion that the need for glycerolipids in the plastids is met by shuffling glycerolipids synthesized in the cytoplasm to the plastids. Cytoplasmic GPAT in the microsomes from leaves can use 18:1- and 16:0-CoA, whereas those from maturing seeds can also use 12:0-, 18:0-, and 22:1-CoA, depending on the plant species. The latter substrate preference is related to the acyl moieties at the *sn*-1 position of storage TAGs in the seeds of individual plant species (Voelker and Kinney, 2001). *GPAT* encoding the cytoplasmic enzymes has been studied recently in Arabidopsis (Zheng et al., 2003). GPAT may be encoded by seven potential *GPAT* genes. Homozygous null mutation of At*GPAT*1 brings deleterious consequences to the tapetum cells, leading to male sterility. It is unknown whether At*GPAT*1 encodes the predominant, ER-located GPAT and whether the other six genes also encode redundant GPATs.

The plastid LPAT from Brassica and Arabidopsis are more active in vitro on 16:0- than 18:1-CoA, a characteristic of the prokaryotic enzyme (Bourgis et al., 1999; Kim and Huang, 2004; Yu et al., 2004). Arabidopsis has only one gene, At*LPAT*1, that encodes the plastid LPAT, and mutational loss of this gene leads to embryo death. The cytoplasmic LPATs in microsomal fractions from several plant species exhibit a substrate preference for 18:1- over 16:0-CoA, a characteristic of the eukaryotic enzyme (Ohlrogge and Browse, 1995). Species in which the seed oils have uncommon acyl moieties at the *sn*-2 position possess additional seed-specific LPATs that are reactive toward the respective uncommon acyl-CoAs (Cao et al., 1990; Laurant and Huang, 1992; Brown et al., 1995; Frentzen, 1998). Genes encoding cytoplasmic LPATs in maturing seeds or other organs from several species, including maize (*Zea mays*) (Brown et al., 1994), coconut (*Cocos nucifera*) (Knutzon et al., 1995), and meadowfoam (*Limnanthes alba*) (Hanke et al., 1995) have been reported. The deduced amino acid sequences of the enzymes contain transmembrane segments indicative of association with membranes, and the enzyme from the leaf or seed extracts can be recovered in the microsomal fraction. However, whether these studied LPATs are located in the ER is unknown. In plants and other organisms, LPAT activities have been found in the microsomes, plasma membrane (Bursten et al., 1991), and mitochondria (Zborowski and Wojtczak, 1969). It is also unknown whether redundant LPATs encoded by different genes exist in an individual plant to perform the same or different physiological functions.

We have examined all the putative At*LPAT* genes in Arabidopsis. Only one gene, At*LPAT*2, encodes the ubiquitous, abundant, and ER-located LPAT. A related gene, At*LPAT*3, is expressed mostly but highly in pollen. A heterozygous mutant of At*LPAT*2 (a null allele, At*lpat*2) has no major altered vegetative growth. However, the presence of At*lpat*2 in the haploid gametophytes leads to the death of the female gametophytes but not the male gametophyte. The survival of the male gametophyte is apparently due to the presence of the abundant AtLPAT3. Here, we report our findings.

RESULTS

Arabidopsis Has Four Putative Cytoplasmic AtLPATs That Can Be Divided into Two Groups

Five Arabidopsis genes (At*LPAT*1-5) could encode LPATs on the basis of their predicted amino acid sequences being similar to those of demonstrated LPATs in other plant and nonplant systems (Kim and Huang, 2004; Yu et al., 2004). Several additional Arabidopsis genes that encode proteins whose amino acid sequences are similar to those encoded by the above putative At*LPAT* genes have recently been shown to encode GPAT (Zheng et al., 2003).

An unrooted phylogenetic tree of the amino acid sequences of proteins derived from At*LPAT*1-5 and closely related genes of other plant species, yeast, and *Escherichia coli* reveals several groups of putative LPATs (Figure 1). One group includes the known plastid (AtLPAT1) and *E. coli* LPAT. Another group comprises the studied microsomal LPATs of several other plant species and AtLPAT2 and 3. A third group consists of AtLPAT4 and 5 and an unstudied rice (*Oryza sativa*) LPAT derived from genomic sequence. A fourth group encompasses the studied

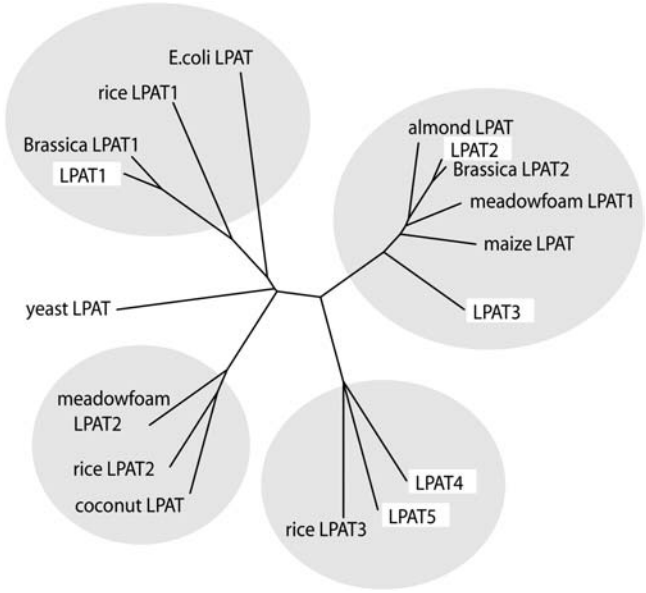

Figure 1. An Unrooted Phylogenetic Tree of Five Putative LPATs of Arabidopsis and Related LPATs of Other Plant Species Constructed on the Basis of Their Predicted Amino Acid Sequences.

The LPATs of *E. coli* and yeast are included for comparison. Genes and proteins were obtained after a BLAST search of the databases of The Arabidopsis Information Resource and National Center for Biotechnology Information with use of the amino acid sequences of maize LPAT (Z29518) and *B. napus* LPAT1 (AF111161) as queries. They were of Arabidopsis (*LPAT*1, At4g30560; *LPAT*2, At3g57650; *LPAT*3, At1g51260; *LPAT*4, At1g75020; *LPAT*5, At3g18850), Brassica (LPAT2, Z95637), rice (LPAT1, AC068923; LPAT2, NM191504; LPAT3, AL606645), meadowfoam (LPAT1, S60478; LPAT2, S60477), coconut (U29657), almond (AF213937), *E. coli* (*pls*C, M63491), and yeast (*slc*1, L13282).

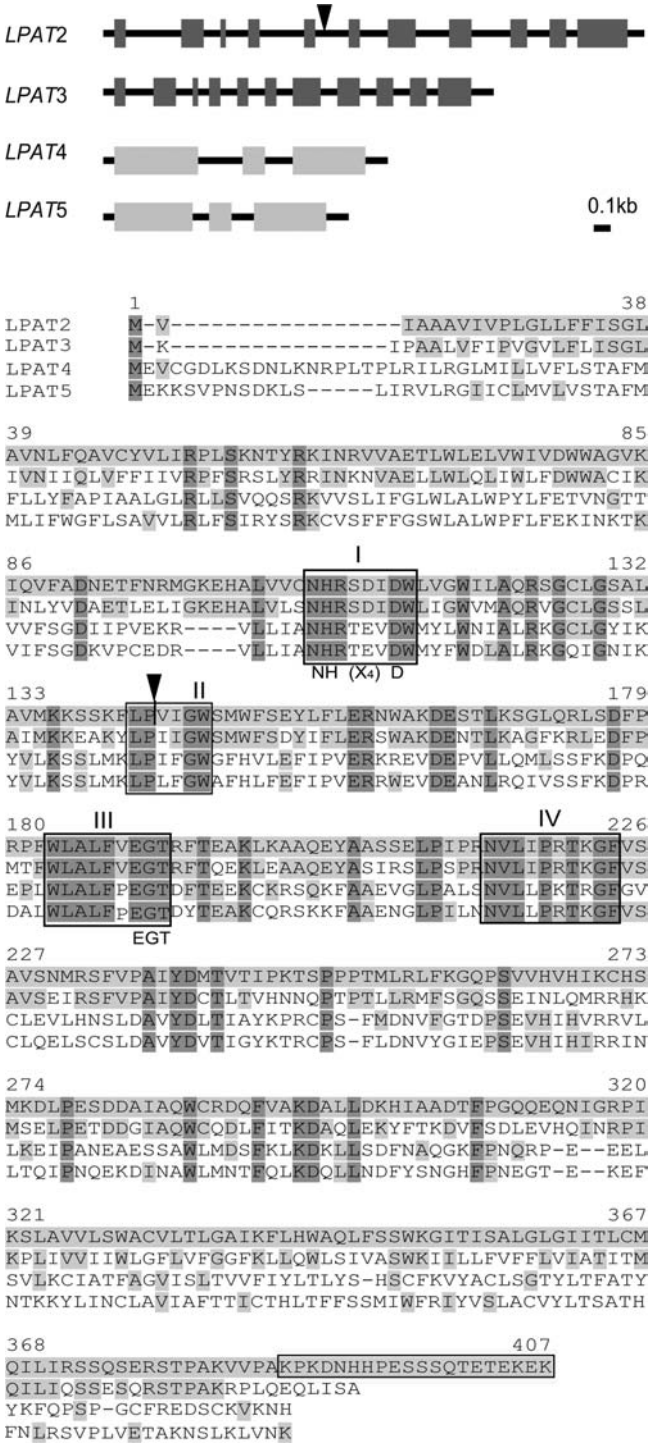

Figure 2. Structures of Four Putative Arabidopsis *LPAT* Genes Encoding Cytoplasmic LPATs and Their Predicted Amino Acid Sequences.

Top panel: the exons (boxes) and introns (lines) of the four genes. Bottom panel: an alignment of their predicted amino acid sequences with the AlignX program from Vector NTI Suite. Residues identical to those in LPAT2 in some of the LPAT3-5 are lightly shaded, and those identical in all four LPATs are heavily shaded. The I [NH(X_4)D], II, III (EGT), and IV motifs conserved in related acyltransferases in various species are boxed. The C-terminal sequence of LPAT2, whose corresponding synthetic polypeptide was used to prepare antibodies, is boxed. The insertion site of T-DNA in *LPAT2* and the corresponding location on LPAT2 are indicated by inverted arrows.

coconut and meadowfoam microsomal LPATs. This last group might represent seed-specific LPATs that can acylate a unique acyl group to the *sn*-2 position of a TAG molecule (Kim and Huang, 2004), such as C-12 in coconut (Oo and Huang, 1989; Knutzon et al., 1995) and C-22:1 in meadowfoam (Cao et al., 1990; Hanke et al., 1995). Nevertheless, this last group also includes a rice LPAT derived from a genomic sequence, and rice seed TAG is not known to possess a unique acyl moiety at the *sn*-2 position. Finally, the yeast LPAT does not have a closely related LPAT in plants.

AtLPAT2-5 (hereafter, the prefix At is omitted for simplicity) can be divided into two groups on the basis of their amino acid sequences. The identity of residues in amino acid sequences is 57% between LPAT2 and 3; 54% between LPAT4 and 5; and 23% or less between the two pairs. LPAT2 and 3 share a similar location of the putative transmembrane segments along the sequences, and this location differs from that shared by LPAT4 and 5 (Kim and Huang, 2004). *LPAT*2 and 3 have a similar pattern of introns, which differs strikingly from that shared by *LPAT*4 and 5 (Figure 2). Yet, the four LPATs all contain the four conserved domains (I to IV) of acyltransferases in diverse organisms, and their genes are all expressed in the plant.

A pileup of the amino acid sequences of LPAT2-5 shows that LPAT2 has a C-terminal sequence absent in the other three LPATs (Figure 2). A synthetic peptide of this unique sequence, absent also in all other Arabidopsis proteins deduced from the complete genome sequence, was used to prepare antibodies against LPAT2.

*LPAT*2 Functionally Complemented an *E. coli LPAT* Mutant, and Its Encoded Protein Synthesized in the Bacteria Had in Vitro LPAT Enzyme Activity

We tested whether *LPAT*2-5 encode proteins that possess LPAT enzymatic activity. *E. coli* JC201, a temperature-sensitive mutant of *LPAT* (Coleman, 1990), was used. The mutant grows at 30°C but not at 42°C. The full-length open reading frame (ORF) of each of the four *LPAT*s was inserted into the expression vector pQE, which contains the T5 promoter transcription-translation system. The resulting pQE-LPAT(2-5) and the control pQE were transformed into JC201, which had been transformed with pREP4 to prevent potential leakiness of the T5 promoter.

Cells containing pQE-LPAT(2-5) grew as well as the wild type containing pQE in the absence of isopropyl-β-thiogalactoside (IPTG) but poorly when IPTG at the low concentration of 0.2 mM was added to the growth medium. Apparently, LPAT2-5 strongly inhibited bacterial growth, a phenomenon that is quite common when eukaryotic membrane proteins are synthesized in transformed bacteria (Laage and Langosch, 2001). We used cells grown in 0.2 mM IPTG overnight to test functional

complementation on an agar plate and for 1 h (when the cells started to express the Arabidopsis *LPAT* and accumulated its LPAT) in a liquid medium to prepare membrane fractions for biochemical analyses.

Figure 3A shows that JC201 harboring either pQE or pQE-LPAT2 grew at 30°C, but only that harboring pQE-LPAT2 grew at 42°C. At 42°C, the colonies were irregularly shaped and fewer than those at 30°C. Thus, LPAT2 was active in vivo and complemented the defective *E. coli* LPAT. Attempts to observe similar functional complementation in JC201 with *LPAT*3, 4, and 5 were unsuccessful, presumably because LPAT3, 4, and 5 were more potent in inhibiting bacterial growth.

Proteins in *E. coli* JC201 harboring pQE and pQE-LPAT2 were analyzed by SDS-PAGE (Figure 3B). Proteins in the membrane fractions from the two bacterial samples separated on the gel had an identical pattern. After immunoblotting, a protein of 45 kD (45,352 D being the expected molecular mass of the 6-His–tagged polypeptide derived from the ORF) in the sample of bacteria harboring pQE-LPAT2 but not that harboring pQE was recognized by anti-LPAT2. The membrane fractions from these two bacterial samples were assayed for LPAT activity with use of LPA-18:1 as the acyl acceptor and either 16:0- or 18:1-CoA as the acyl donor (Figure 3C). The membrane fraction from bacteria harboring pQE had minimal enzymatic activity, which was higher with 16:0-CoA than with 18:1-CoA, a characteristic of the prokaryotic enzyme (Ohlrogge and Browse, 1995); the activity should represent that of the native bacterial enzyme. The membrane fraction from bacteria harboring pQE-LPAT2 had several hundred times higher LPAT activity, and the activity was higher with 18:1-CoA than 16:0-CoA, a characteristic of the eukaryotic (cytoplasmic) enzyme (Ohlrogge and Browse, 1995); the activity should represent mostly LPAT2 activity. Attempts to observe similar in vitro enzymatic activities in LPAT3, 4, and 5 in the transformed bacteria were largely unsuccessful. The membrane fraction from bacteria harboring pQE-LPAT3 had LPAT activity, which was two to three times higher than that in the membrane fraction from bacteria harboring pQE and preferred 18:1-CoA over 16:0-CoA (Figure 3C). This acyl-CoA preference should reflect largely that of LPAT3 and not the native bacterial enzyme. The membrane fraction from bacteria harboring pQE-LPAT4 and 5 had only background (bacterial) activity that was higher with 16:0-CoA than with 18:1-CoA (data not shown).

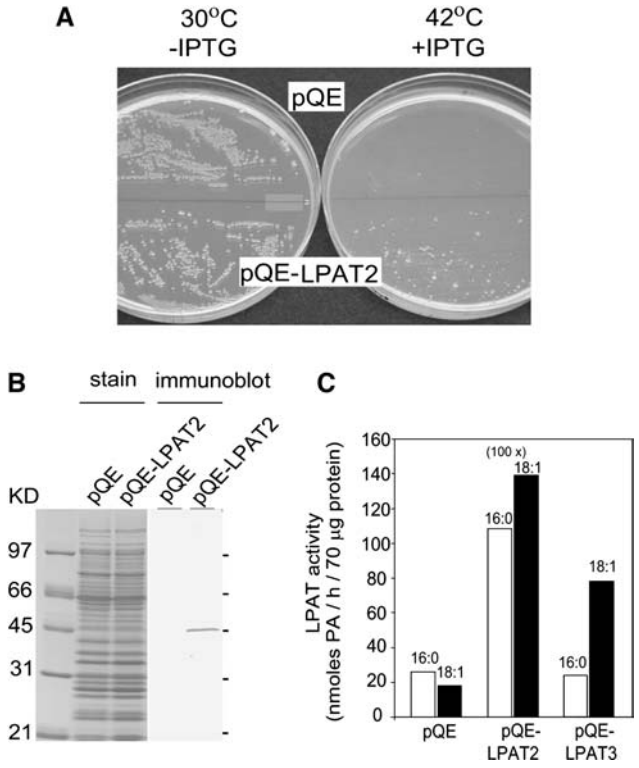

Figure 3. Expression of *LPAT*2 and *LPAT*3 in the *E. coli* Strain JC201, a Temperature-Sensitive Mutant Defective in *LPAT*.

(A) Bacteria transformed with pQE, pQE-LPAT2, or pQE-LPAT3 were grown at 30° C or 42° C for 18 h and photographed. pQE-LPAT2 (shown) but not pQE-LPAT3 (data not shown) complemented the mutation.

(B) Membrane fractions of bacteria transformed with pQE or pQE-LPAT2 grown at 30°C were analyzed for their protein constituents by SDS-PAGE (left) followed by immunoblotting with antibodies against LPAT2 (right). The antibodies recognized a single recombinant LPAT2 protein of 45 kD. Molecular mass markers are on the left lane.

(C) Membrane fractions from the three types of transformed bacteria were assayed for LPAT activities with the use of equal amounts of protein (70 μg), LPA-18:1, and either 18:1- or 16:0-CoA.

LPAT2 and 3, but Not LPAT4 and 5, Synthesized in Yeast Had in Vitro LPAT Enzyme Activities

LPAT2-5 synthesized in transformed *E. coli* apparently inhibited bacterial cell growth. Inhibition of fungal cell growth was not observed when *LPAT*2-5 were transformed into and expressed in yeast. *LPAT* was placed in the yeast-transforming plasmid pYES under the control of the *GAL*1 promoter, which can be activated with galactose and to a lesser extent glucose (Giniger et al., 1985). Grown in glucose, yeast harboring pYES-LPAT contained the *LPAT* transcript at a low level (Figure 4A). Four hours after the addition of galactose to the growth medium, the yeast possessed several times more of the *LPAT* transcript. The total lysate of the yeast harboring pYES-LPAT resolved on a SDS-PAGE gel possessed a protein band of ~43 kD (Figure 4B), which is the deduced molecular mass of LPAT2-5. The ~43-kD protein band was also present in the lysate of yeast transformed with pYES. The yeast genome has genes that could encode 132 unmodified proteins of 42 to 44 kD (http://db.yeastgenome.org), and the lone yeast LPAT has 34 kD. Therefore, the ~43-kD protein band in the lysate of the yeast harboring pYES-LPAT should represent non-LPAT proteins of the yeast and LPAT2-5. LPAT2 in the 43-kD protein band from the lysate of yeast transformed with *LPAT*2 was positively identified with antibodies against an LPAT2-specific polypeptide. The amount of LPAT2 was higher in the transformed yeast grown in galactose than in glucose (Figure 4C), consistent with the level of the *LPAT*2 transcript (Figure 4A). Yeast lysate containing LPAT2 or 3 showed in vitro LPAT activities substantially higher than that in the control lysate of yeast transformed with pYES, whereas those

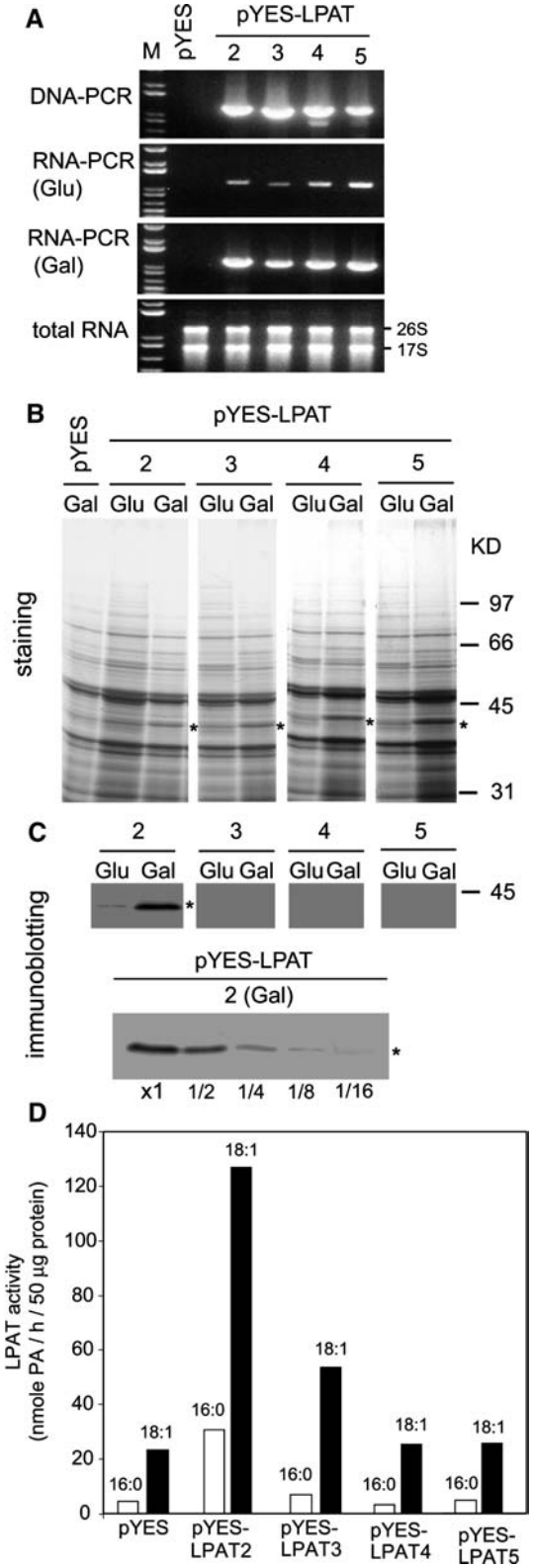

Figure 4. Expression of *LPAT*2-5 in *Saccharomyces cerevisiae*.

(A) Yeast transformed with pYES or pYES-LPAT2-5 were analyzed for the presence of *LPAT*2-5 in DNA (cells grown in glucose) and *LPAT*2-5 transcripts in RNA (cells grown in glucose [Glu] and then transferred to a galactose medium and grown for 4 h [Gal]) by PCR. Samples containing approximately equal amounts of total RNA (shown) were used in the RT-PCR.

(B) Lysates of the transformed yeast were analyzed for protein constituents by SDS-PAGE. Asterisks indicate the protein band containing LPAT2-5; the band also contained other yeast proteins because it was also present in the lysate of yeast transformed with pYES.

(C) SDS-PAGE immunoblotting of membrane fractions of transformed yeast grown in glucose and then galactose for 4 h (top); the antibodies were raised against a synthetic peptide unique to LPAT2. Sensitivity of the immunoblotting was shown with decreasing amounts of the sample from galactose-grown yeast transformed with *LPAT*2 (bottom). Positions of molecular mass markers are shown at the right in **(B)** and **(C)**.

(D) Lysates of the transformed yeast grown in glucose and then galactose for 4 h were analyzed for LPAT activities with the use of equal amounts of protein (50 µg) and LPA-18:1 and either 18:1- or 16:0-CoA.

containing LPAT4 and 5 had activities similar to those in the control yeast lysate (Figure 4D). Both LPAT2 and LPAT3, as well as the yeast native LPAT, had activities higher with 18:1-CoA than with 16:0-CoA, a characteristic of the eukaryotic enzyme. These findings on LPAT2-5 synthesized in yeast are consistent with those in *E. coli*.

The *LPAT*2 Transcript Was the Most Abundant and Ubiquitous, the *LPAT*3 Transcript Was Abundant in Pollen, and the *LPAT*4 and 5 Transcripts Were Ubiquitous but Scarce

Three different methods were used to study the prevalence of the *LPAT*2-5 transcripts. Each method has its advantages and uncertainties, but together they would produce complementary results revealing a general theme.

RT-PCR results show that the *LPAT*2, 4, and 5 transcripts were present in all of the five organs examined: siliques, inflorescences, rosette leaves, stems, and roots (Figure 5). The *LPAT*3 transcript was detected in only inflorescences and roots. In addition, the *LPAT*2, 4, and 5 transcripts but not the *LPAT*3 transcript were detected in developing embryos, whereas all were present in seedlings. The *LPAT*3 transcript was apparently more abundant than the *LPAT*2 transcript in pollen (Figure 5). Although this RT-PCR result with pollen is at best semiquantitative, it is consistent with the findings of the β-glucuronidase gene (*GUS*) expression (to be described in Figure 7). It is also consistent with the reported transcriptomes of the Arabidopsis pollen, where *LPAT*3 and not *LPAT*2, 4, and 5 was present in abundance (Becker et al., 2003; Honys and Twell, 2003).

The recently available massively parallel signature sequencing (MPSS) database of Arabidopsis (Meyers et al., 2004) was used to assess the prevalence of the *LPAT*2-5 transcripts. This 17-mer MPSS database of a reasonable size (2 to 4 million signature sequences from each cDNA library) was constructed with *Sau*3A restriction fragmentation, and the ORFs of *LPAT*2-5 have 3, 5, 4, and 3 *Sau*3A sites, respectively. Thus, a comparison of the prevalence of the four transcripts in the MPSS

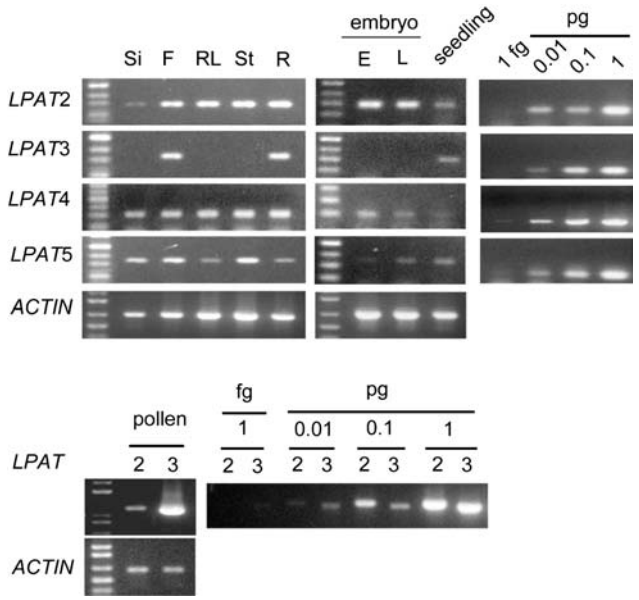

Figure 5. RT-PCR Analyses of the Transcripts of *LPAT*2-5 in Various Organs.

The organs included siliques (Si), unopened flowers (F), rosette leaves (RL), stems (St), roots (R), and early (E) and late (L) maturing embryos and seedlings. The bottom panel shows a comparison of the levels of *LPAT*2 and 3 transcripts in mature pollen. Approximately equal amounts of transcripts of an Arabidopsis actin gene (*ACTIN*) were present in the various samples. The lengths of the RT-PCR fragments are those expected from the primers used. The RT-PCR products were obtained with primers and cycle numbers at a linear range, as revealed in the results of DNA-PCR with use of increasing amounts of full-length *LPAT* cDNA and the same primers and cycle numbers.

database should provide an approximation. Figure 6 shows that in all of the five examined organs, the *LPAT*2 transcript was substantially more abundant than all the other three transcripts combined.

The promoter regions of the four *LPAT*s were each attached to the reporter gene *GUS*, and the constructs were transformed into Arabidopsis plants. GUS activity in the various organs of the transformed plants was examined (Figure 7). It was highest in the veins of leaves, inflorescence stalks, and roots when *GUS* was driven by the *LPAT*2, 4, and 5 promoters. GUS activity was detected mostly in pollen when *GUS* was driven by the *LPAT*3 promoter. In pollen, the *LPAT*3 promoter appeared to be more active than the *LPAT*2 promoter, whereas *LPAT*4 and 5 promoters were totally inactive in driving the expression of *GUS* (Figure 7). This observation of the relative strength of the *LPAT*2 and 3 promoters in driving *GUS* in pollen is consistent with the RT-PCR results (Figure 5). In the pistil, GUS activity in the female gametophyte was detected only when *GUS* was driven by the *LPAT*2 promoter; it was clearly detected at the four-nucleate stage and increased to a maximum at the eight-nucleate stage and then declined after fertilization (Figure 7). This decline could be due to dilution of the *GUS* transcript or protein as a result of cell multiplication.

Overall, results obtained from the above three different methods reveal a general theme of the expression of the four *LPAT*s. The *LPAT*2, 4, and 5 transcripts are ubiquitous, but the *LPAT*2 transcript dominated. *LPAT*3 is expressed mostly in pollen, where its transcript is more abundant than the *LPAT*2 transcript and where the *LPAT*4 and 5 transcripts are absent. The *LPAT*2 transcript is the only one present in the female gametophyte.

LPAT2 Was Ubiquitous and Located in the ER

Antibodies against a synthetic peptide corresponding to the C terminus of LPAT2 were raised. This C-terminal sequence in LPAT2, or a similar version, is absent in LPAT3-5 (Figure 2) and all other Arabidopsis proteins deduced from the genome sequence. The antibodies reacted with LPAT2 but not LPAT3-5 synthesized in transformed yeast (Figure 4C). They detected LPAT2 as a single protein band by SDS-PAGE immunoblotting in the total extracts of all examined Arabidopsis organs, including siliques, floral buds, stems, leaves, and roots (Figure 8B). Thus, LPAT2 was ubiquitous, as was the *LPAT*2 transcript (Figure 5). Anti-LPAT2 antibodies also recognized *Bn*LPAT2 in *Brassica napus* anthers (Figure 8B).

We tested whether LPAT2 was present in the ER or other subcellular compartments. We chose the tapetum cells of Arabidopsis and Brassica, in which the ER is abundant and the interfering autofluorescent chloroplasts are absent (Platt et al., 1998), to study localization. Double labeling with antibodies against LPAT2 and the ER marker calreticulin shows

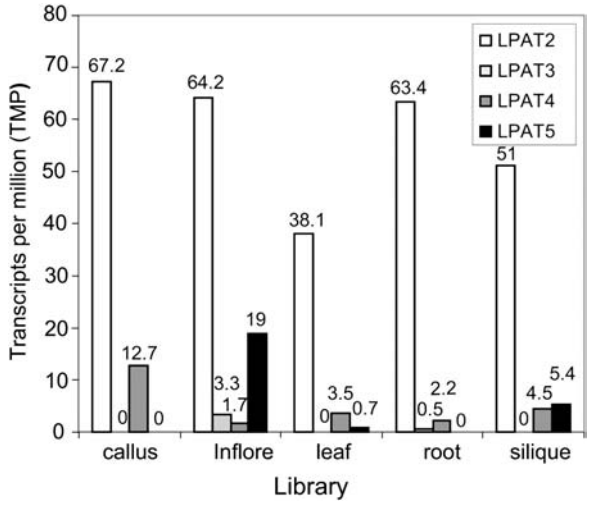

Figure 6. Transcripts of the Four Putative Genes in Different Organs with Use of the MPSS Database.

Information was obtained from http://mpss.udel.edu/at (Meyers et al., 2004). Signature sequences of 17 nucleotides of each gene in five different libraries are shown. The signatures of 17-mer tags generated via cutting the cDNA in the libraries at the *Sau*3A restriction sites were normalized to transcripts per million to facilitate comparisons among libraries.

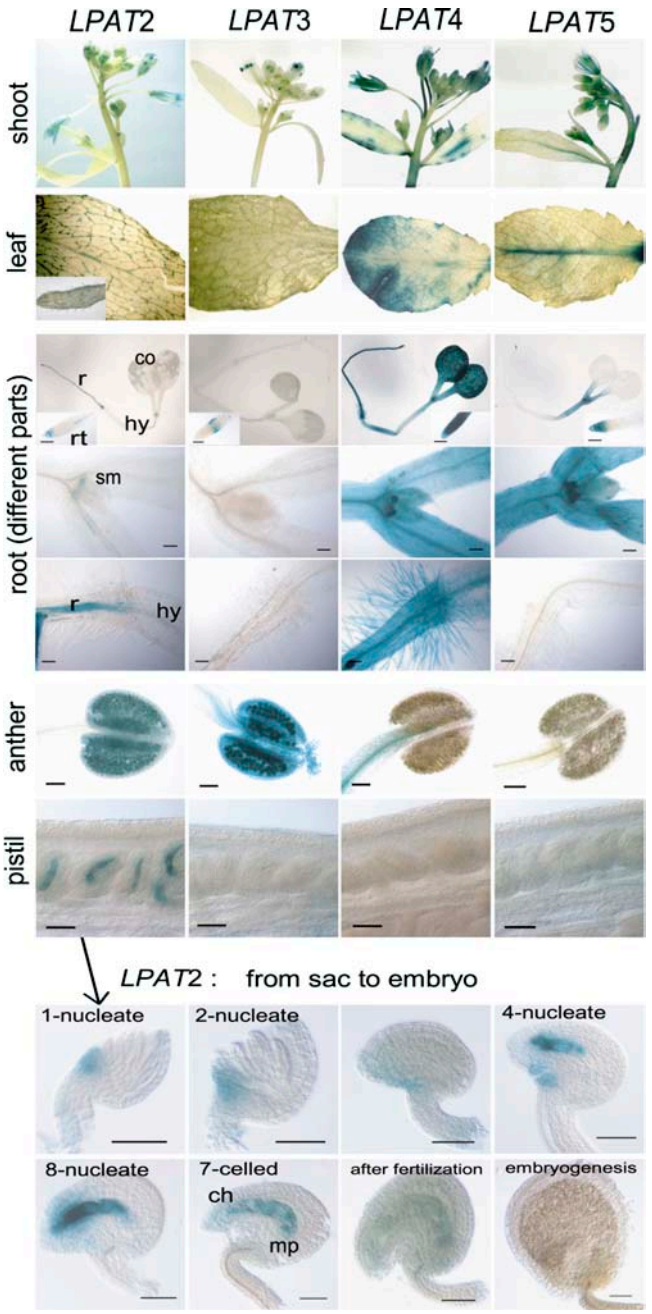

Figure 7. GUS Activities in Different Parts of Arabidopsis Plants Transformed with a Construct Containing the Promoter of *LPAT2*-5 Ligated to the ORF of a *GUS* Gene.

The bottom panel details GUS activities from *GUS* driven by the *LPAT2* promoter in the ovule during development before and after fertilization. Bars represent 50 μm in the root, 20 μm in the anther and pistil, and 10 μm in the ovule samples. ch, chalazal pole; co, cotyledon; hy, hypocotyl; mp, micropylar pole; r, root; rt, root tip; sm, shoot meristem.

that in Arabidopsis tapetum cells, LPAT2 was largely colocated with calreticulin (Figure 8C). Small regions in the ER were not occupied by either LPAT2 or calreticulin, and the existence of these nonoverlapping regions reaffirms the presence of specialized subdomains in the ER (Papp et al., 2003). Similar colocation of BrLPAT2 and calreticulin was observed in Brassica tapetum cells (Figure 8C). Results of control experiments with antibodies against other organelle markers reaffirm that BrLPAT2 was colocated with calreticulin in the ER in Brassica tapetum cells. For example, the plastid protein, plastid lipid–associated protein (Kim et al., 2001), was localized in the plastids independent of the calreticulin in the ER (Figure 8C).

Complementary data supporting the presence of LPAT2 in the ER were obtained by subcellular fractionation of Brassica sporophytic anther extract followed by SDS-PAGE and immunoblotting (Figure 8D). LPAT2 and calreticulin were colocalized in the 100-k*g* (the microsomes) and the 10-k*g* pellets, whereas the plastid lipid-associated proteins were present mostly in the 10- and 1-k*g* pellets.

A Heterozygous (*LPAT2*/*lpat2*) Mutant Possessed Half of the *LPAT2* Transcript and LPAT and No Greatly Altered Leaf Acyl Composition or Vegetative Morphology

Seeds containing T-DNA–inserted *LPAT2* (*lpat2*) were studied (Salk_058130, T-DNA inserted into At3g57650). Of the plants grown from the 13 seeds we obtained, eight were wild type (*LPAT2*/*LPAT2*) and five heterozygous mutants (*LPAT2*/*lpat2*). All these heterozygous mutants shared the same vegetative and reproductive morphology, and we will describe one in detail. The heterozygous mutant had only one copy of T-DNA inserted into its genome, as evidenced by DNA gel blot results (Figure 9). Leaf DNA was cut with *Pst*I, whose sites are present in the T-DNA and at the opposite ends of *LPAT2*. Fragments on the blot were hybridized with a 1.6-kb DNA probe, which represents the 5′-terminus of *LPAT2* (1.2 kb) and the 5′-terminus of the T-DNA (0.4 kb) (to be shown as fragment a in Figure 10A). The wild-type DNA had only one *Pst*I fragment of the expected 2.8 kb. The heterozygous mutant DNA had an additional ~5.4-kb *Pst*I fragment, which represents the 1.2-kb 5′-terminus of *LPAT2* and ~4-kb 5′ terminus of the T-DNA.

RNA gel blot analysis of the leaf RNA from the mutant and the wild type was performed with the probe used for the above-mentioned DNA gel blot analysis (Figure 9). The heterozygous mutant contained the wild-type *LPAT2* transcript of 1.4 kb of approximately half the amount in the wild type and another fragment of 1.3 kb, which could represent a truncated *LPAT2* transcript. The leaves of the heterozygous mutant also had approximately half of the LPAT2 present in the wild type (Figure 8A).

The heterozygous mutant was similar to the wild type in vegetative morphology (Figure 9), except that its rosette leaves were slightly shorter. Its leaf acyl composition was also similar to that of the wild type, possessing 18:3, 18:2, 16:0, 16:3, and 16:1 as the abundant acyl moieties (data not shown).

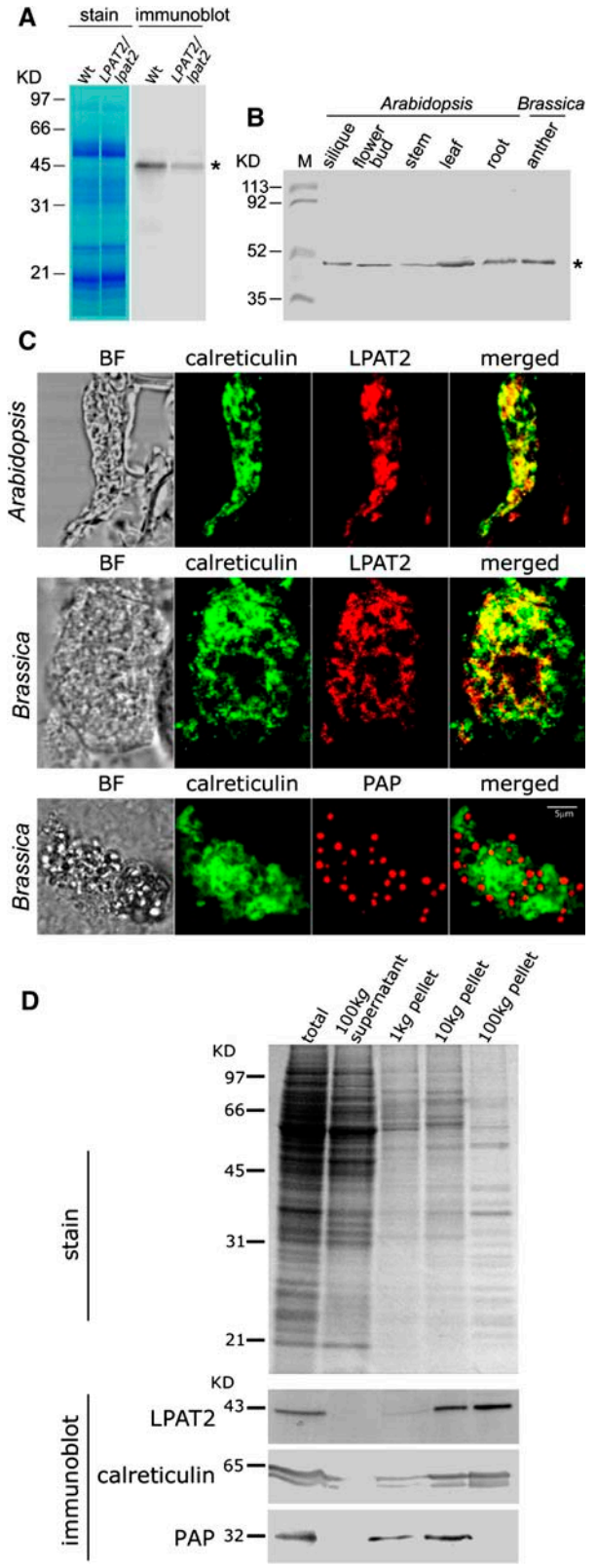

Figure 8. Detection of LPAT2 in Extracts of Different Organs and Its Localization in the ER of the Tapetum Cells of Arabidopsis and Brassica.

The Heterozygous (*LPAT2*/*lpat2*) Mutant Produced Shorter Siliques That Contained Half Normal Seeds and Half Remnants of Aborted Ovules

Although the heterozygous mutant was similar to the wild type in vegetative growth, it was not so in its reproductive growth (Figure 9). Its mature siliques were approximately two-thirds the length of those in the wild type. They contained approximately half normal-sized seeds and half empty slots filled with apparently aborted ovules that had not been fertilized. No seed or ovule of an intermediate size indicative of abortion after fertilization was observed. The aborted ovules in the siliques could be recognized soon after fertilization of the flowers 4 d after flowering (DAF) because they did not increase in size, whereas the fertilized ovules continued to do so. Sections of the ovules before fertilization reveal that the *lpat2* female gametophyte began to differ from that of the wild type at the four-cell stage (Drews and Yadegari, 2002). At this stage, the central cell of the wild type contained abundant ER, whereas that of the *lpat2* mutant had numerous large starch grains (Figure 9). The presence of abundant ER in the central cell of the wild type indicates the need of abundant membranes and ER activities; thus, a loss of LPAT2 in the *lpat2* female gametophyte is deadly. In the *lpat2* central cell, the reduced carbon designated for the ER membrane activities might have been channeled to form the starch granules. The wild-type egg cell did not contain abundant ER but was packed with different organelles and a large vacuole. The *lpat2* egg cell also had similar subcellular structures, although its membrane structures in general were less defined (data not shown). Thus, the abortion of the *lpat2* female gametophyte before or immediately after fertilization could have been caused by the absence of LPAT2 in the egg cell (which would become the embryo after fertilization), the central cell (which would become the endosperm), or both cells. It is known that the endosperm is required for successful embryogenesis, and aborted endosperm leads to death of the embryo regardless of whether the

(A) An SDS-PAGE gel of the total leaf extracts from the wild type and the heterozygous mutant (*LPAT2*/*lpat2*) and an identical gel after immunoblotting with anti-LPAT2.

(B) LPAT2 in the total extracts of different organs analyzed by SDS-PAGE and then immunoblotting. In **(A)** and **(B)**, the asterisk denotes the recognized LPAT2.

(C) Immunofluorescence microscopic images of double-labeled Arabidopsis and Brassica tapetum cells. The image of each cell was observed by bright-field (BF) microscopy and immunofluorescent microscopy labeled with antibodies against LPAT2, calreticulin (ER marker), and plastid lipid associated protein (PAP; plastid marker). All images are of the same magnification. Bar = 5 μm.

(D) An SDS-PAGE gel of the total sporophytic anther extract from Brassica and its subfractions by centrifugations and identical gels that had been subjected to immunoblotting with antibodies against the indicated proteins. Two protein bands of 50 to 60 kD were recognized by antibodies against castor bean (*Ricinus communis*) calreticulin. The amounts of the various subfractions loaded to the gel corresponded to those from the same amount of the total extract. In all gels, positions of molecular mass markers are shown at the left.

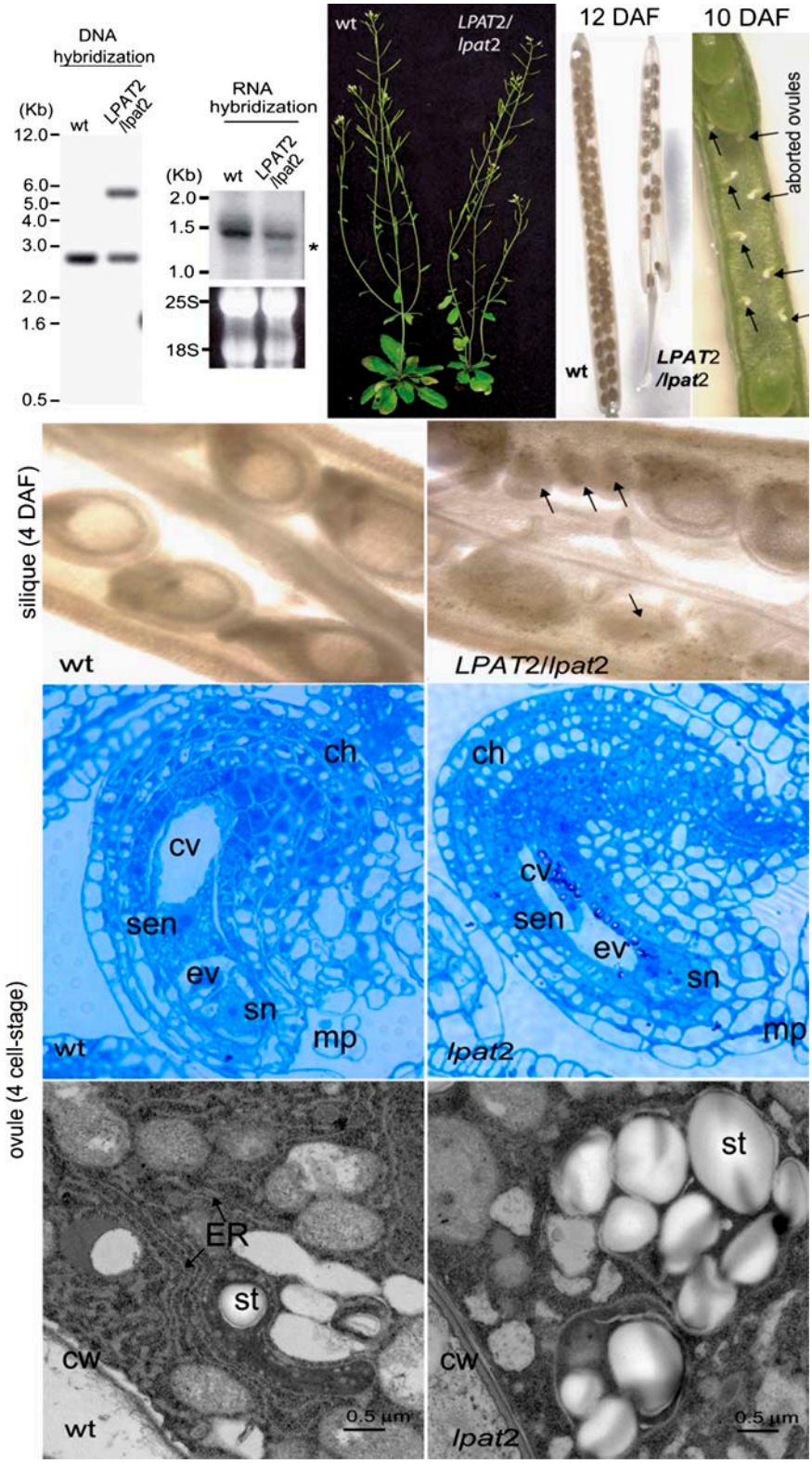

Figure 9. Comparisons of the Heterozygous Mutant (*LPAT2*/*lpat2*) with the Wild Type (*LPAT2*/*LPAT2*).

DNA hybridization shows that both plants contained the *Pst*I fragment of *LPAT2* (2.8 kb), whereas the mutant also had the *Pst*I fragment of *lpat2* (5.4 kb). RNA hybridization reveals that the mutant had approximately half the *LPAT2* transcript (1.4 kb) of the wild type and a transcript of 1.3 kb that could

embryo is initially viable (Costa et al., 2004). The sporophytic cells enclosing the gametophyte in both the mutant and wild type at the four-cell stage appeared to be similar.

Results of Segregating *lpat2* after Selfing the Heterozygous Mutant or Crossing It with the Wild Type Reveal Deleterious Effect of *lpat2* in the Female Gametophyte

Results of reciprocal crossing between the heterozygous *LPAT2*/*lpat2* mutant and the wild type support the notion that *lpat2* causes ovule rather than embryo or pollen lethality (Table 1). Selfing of the heterozygous mutant produced siliques containing half of the number of seed per silique (compared with that in the wild type) and empty slots (approximately the same number as the slots filled with seed) possessing aborted ovules (Figure 9, Table 2). This 1:1 ratio is indicative of inheritance of the female or male gametophyte (Drews and Yadegari, 2002). Results of genetic crossing reveal that the deleterious effect of *lpat2* was exerted only at the female gametophyte. Crossing the heterozygous mutant as the female with wild-type pollen also produced siliques that contained half of the number of seeds per silique as that in wild-type siliques. Plants grown from 20 of these seeds were found to be all of the *LPAT2*/*LPAT2* genotype. Crossing the wild type as the female with pollen from the heterozygous mutant produced siliques that contained the same number of seeds as that in wild-type siliques. Plants grown from 20 of these seeds were examined; 10 had the *LPAT2*/*LPAT2* genotype and 10 the *LPAT2*/*lpat2* genotype.

In summary, we conclude that *lpat2* causes lethality in the female gametophyte on the basis of the following findings. First, LPAT2 is the only LPAT in the female gametophyte because the promoter of *LPAT2* but not *LPAT3-5* drove the expression of *GUS* in the female gametophytes of transformed plants (Figure 7). Second, the central cell of the *lpat2* female gametophyte at the four-cell stage began to differ from that of the wild type in possessing numerous starch grains instead of abundant ER, consistent with the loss of LPAT that is essential for phospholipid synthesis (Figure 9); less obvious but noticeable changes in the membranes in the *lpat2* egg cell also occurred. Third, results of reciprocal crossing of the heterozygous mutant with the wild type provide genetic evidence for female and not male gametophytic lethality (Table 1). We speculate that *lpat2* did not cause pollen lethality because the more abundant LPAT3 there compensated for the loss of LPAT2.

LPAT2-cDNA Functionally Complemented *lpat2* in Heterozygous (*LPAT2*/*lpat2*) and Homozygous (*lpat2*/*lpat2*) Mutants

The above-mentioned phenotypes of the *lpat2* mutant were caused solely by a T-DNA insertion into *LPAT2*, as evidenced by the successful rescue of the mutation after the heterozygous mutant was transformed with the *LPAT2*-promoter:*LPAT2*-cDNA (abbreviated as *LPAT2*P:*LPAT2*-c). Five of the T2 plants were heterozygous (*LPAT2*/*lpat2*) and contained *LPAT2*, *lpat2*, and *LPAT2*-c (Figure 10A). They produced 81% of the seeds per silique as that of the wild type; this proportion is substantially higher than the 46% produced by the untransformed heterozygous plant (Table 2). Four of the T2 plants were homozygous (*lpat2*/*lpat2*) and contained *lpat2* and *LPAT2*-c (Figure 10A). They produced 85% of the number of seeds per silique as that of the wild type; again, this proportion is substantially higher than the 46% produced by the untransformed, heterozygous plant (Table 2). We never found the genotype *lpat2*/*lpat2* in the offspring from selfing the untransformed heterozygous mutant.

LPAT3-cDNA Functionally Complemented *lpat2* in Part in Heterozygous (*LPAT2*/*lpat2*) and Homozygous (*lpat2*/*lpat2*) Mutants

Pollen of the genotype *lpat2* were viable and could fertilize eggs (Table 1). We speculate that *LPAT3*, whose transcript was abundant in pollen, compensated for the loss of *LPAT2*. Recombinant LPAT3 produced by *E. coli* (Figure 3) and yeast (Figure 4) had LPAT activity in vitro. We tested whether *LPAT3*-c could functionally complement *lpat2* in the ovules by transforming the heterozygous mutant (*LPAT2*/*lpat2*) with *LPAT2*P:*LPAT3*-c. The shoots and roots of several transformed *LPAT2*/*lpat2* mutants contained *LPAT2* in amounts similar among themselves and to the wild type (Figure 10B). They contained *LPAT3* in amounts substantially higher than those in the shoots (not detectable) and roots (a low amount) of the wild type. Thus, *LPAT3* driven by the *LPAT2* promoter was expressed properly in the shoots and roots of the *LPAT2*/*lpat2* mutants. The T3 plants (*LPAT2*/*lpat2* + *LPAT2*P:*LPAT3*-c) were selfed, and the seeds produced from five selfed T3 lines were analyzed (Table 3). The mature siliques produced by these lines were intermediate in length between those of the wild type and the heterozygous mutant (Figure 10C). They contained three distinguishable types of seeds, aborted seeds, or ovules

Figure 9. (continued).

represent the truncated *lpat2* transcript (marked with an asterisk). Approximately equal amounts of the 25S and 18S rRNA (stained with ethidium bromide) were present in the mutant and wild-type samples. The mutant and wild type had similar vegetative morphology. The siliques produced by the mutant were shorter than those of the wild type. During maturation at 4, 10, and 12 DAF, the siliques contained half maturing seeds and half apparently aborted ovules (arrows). Sections of the pistils observed under a light microscope (stained with tuluidine blue, panel second to the bottom) show that the *lpat2* female gametophyte at the four-cell stage in the mutant ovule differed from that of the wild type in having numerous, large, purple starch granules in the central cell. The sporophytic cells enclosing the gametophyte in both the mutant and wild type appeared to be similar. Sections of the central cells observed under an electron microscope (bottom panel) show that the cytoplasm of the *lpat2* female gametophyte contained numerous large starch granules (st) in amyloplasts instead of abundant ER as the wild type did. ch, chalazal pole; cv, central cell vacuole; cw, cell wall; en, egg nucleus; ev, egg vacuole; mp, micropylar pole; sen, secondary endosperm nucleus; sn, synergid cell nucleus.

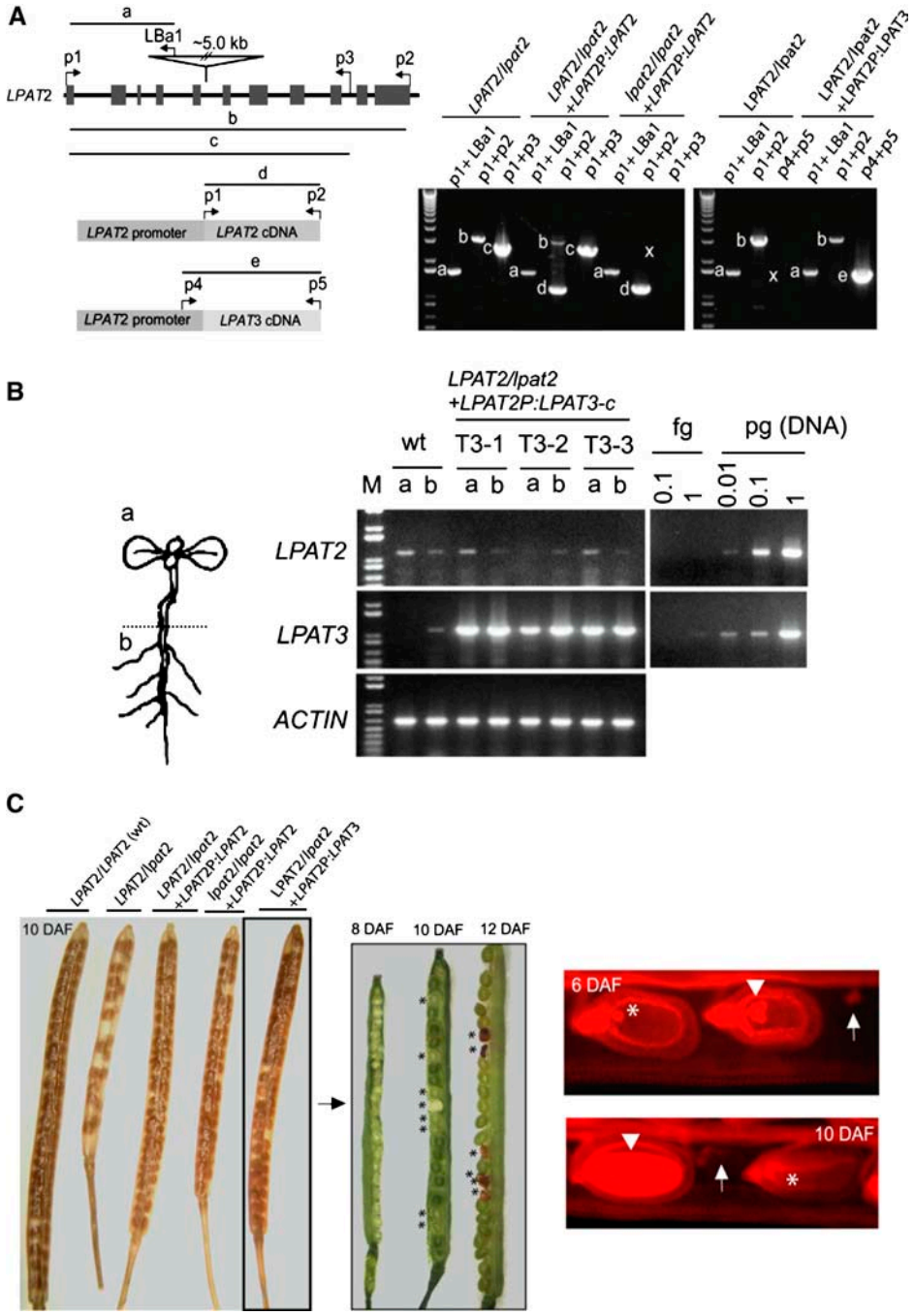

Figure 10. Analyses of the Offspring of *LPAT2*/*lpat2* Transformed with *LPAT2* or *LPAT3*.

(A) The structures of *LPAT2*, *lpat2*, *LPAT2*P:*LPAT2*-c, and *LPAT2*P:*LPAT3*-c and results of PCR genotyping. The primers used and the expected PCR fragments from the DNA are shown. *LPAT2* contains introns (lines) and exons (boxes). The gene *lpat2* contains a T-DNA (inverted triangle with the left border, LBa1) inserted into *LPAT2*. Results of PCR with use of the indicated primers are shown; X indicates the location of the missing fragment on the gel.

(B) RT-PCR analysis of *LPAT2* and *LPAT3* transcripts in 10-d-old shoots (a) and roots (b) of the wild type and *LPAT2*/*lpat2* mutants (T3-1, 2, and 3) transformed with *LPAT2*P:*LPAT3*-c. Approximately equal amounts of transcripts of an Arabidopsis gene (*ACTIN*) were present in the various samples. The RT-PCR products were obtained with primers and cycle numbers at a linear range, as revealed in the results of DNA-PCR with use of increasing amounts of full-length *LPAT* cDNA and the same primers and cycle numbers. M represents RNA length markers.

(C) Images of the siliques from the various genotypes at the indicated DAF. The siliques were treated with ethanol (thus turned brown) for easy observation of the seeds. Green siliques produced by transformed plants (*LPAT2*/*lpat2* + *LPAT2*P:*LPAT3*-c) at 8, 10, and 12 DAF are also shown;

Table 1. Seed Production from Selfing the Heterozygous Arabidopsis Mutant (*LPAT2*/*lpat2*) and Crossing It with the Wild-Type Plant

Crossing	Predicted Genotypes in Gametophytes		Average No. of Seeds/Silique (n = Siliques Counted)	Percentage of Wild Type
	Female	Male		
Wild type selfing	*LPAT2* and *LPAT2*	*LPAT2* and *LPAT2*	51 ($n = 25$)	100
LPAT2/*lpat2* selfing	*LPAT2* and *lpat2*[a]	*LPAT2* and *lpat2*	24 ($n = 25$)	50 ($P < 0.05$)
Female: *LPAT2*/*lpat2* Male: wild type	*LPAT2* and *lpat2*	*LPAT2* and *LPAT2*	18[b] ($n = 5$)	50 ($P < 0.05$)
Female: wild type Male: *LPAT2*/*lpat2*	*LPAT2* and *LPAT2*	*LPAT2* and *lpat2*	44[b] ($n = 5$)	100 ($P < 0.05$)

[a] Underlined genotype indicates predicted nonviability.
[b] Hand crossing produced ~85% fertilization in comparison with natural selfing, which produced 100% fertilization.

(Figure 10C). The first type appeared to be normal, maturing seed, having a heart-shaped embryo at 6 DAF and a fully formed embryo at 10 DAF. These seeds should have the genotypes of *LPAT2*/*LPAT2* or *LPAT2*/*lpat2* plus or minus *LPAT2*P:*LPAT3*-c. The second type was immature seeds containing an aborted embryo, which had reduced development compared with the maturing, normal embryos at 6 and 10 DAF. These aborted seeds did not germinate. They might have derived from *lpat2* + *LPAT2*P:*LPAT3*-c female gametophytes fertilized with pollen of the genotype *LPAT2* or *lpat2* plus or minus *LPAT2*P:*LPAT3*-c. The third type was white ovules that apparently had not been fertilized. The female gametophytes of these aborted ovules could have the genotype of *lpat2* without *LPAT2*P:*LPAT3*-c. The normal seeds, aborted seeds, and aborted ovules were in the ratio of 54:34:12. Although it is difficult to pinpoint the genotypes of these seeds and ovules, it is apparent that *LPAT3*-c allowed ovules of the genotype *lpat2* to survive and be fertilized but did not allow the fertilized ovule to undergo full maturation into seeds.

DISCUSSION

LPAT catalyzes an essential step in the synthesis of glycerolipids. In Arabidopsis, several genes have been speculated to encode LPATs. We have now characterized all these genes. Only one gene each encodes the ubiquitous and abundant LPAT of the plastid and the cytoplasmic systems. *LPAT1* encodes the lone plastid LPAT. Although the *LPAT1*/*lpat1* heterozygous mutant (*lpat1* being a null allele) shows no altered phenotype, the homozygous mutant dies during embryo development (Kim and Huang, 2004; Yu et al., 2004). *LPAT2* encodes the ER-located, ubiquitously distributed LPAT2 (this report). Its transcript is present in all parts of the sporophyte and both gametophytes. Thus, LPAT2 synthesizes glycerolipids in the cytoplasm of all cells and could be essential to cell survival. Although the *LPAT2*/*lpat2* heterozygous mutant (*lpat2* being a null allele) shows little altered phenotype, it produces offspring of a genotypic pattern (Drews and Yadegari, 2002) that is indicative of the death of the *lpat2* female gametophytes. However, the *lpat2* male gametophyte in pollen is viable. In pollen, the related LPAT3 exists, and the *LPAT3* transcript is more abundant than the *LPAT2* transcript. Thus, LPAT3 could rescue the *lpat2* male gametophyte. *LPAT3* is highly expressed in pollen but not at all in most sporophytic parts and the female gametophyte. We suggest that *LPAT3* evolved from an ancestor of *LPAT2* to accommodate the high demand for membrane synthesis in pollen. In pollen, extensive membrane synthesis occurs during tube growth, when widespread vesicle formation, fusion, and breakdown occur for the rapid advancement of the tube (Mascarenhas, 1993).

The *lpat2* female gametophyte transformed with *LPAT3* survived and underwent fertilization, but the embryo could not fully mature. The failure of LPAT3 to rescue the embryo completely could be due to LPAT3 not being an efficient catalytic enzyme, not having an appropriate substrate specificity to produce PA for the various cells of the embryo, or not being able to interact with other proteins on the ER to form effective enzyme complexes. LPAT3 is relatively distinct from LPAT2 of Arabidopsis and other species in amino acid sequence (Figure 1) and may have slightly different molecular characteristics.

We have suggested that the flow of glycerolipids from the cytoplasm to the plastids is limited because the At*lpat1* homozygous mutant having no plastid LPAT1 cannot be rescued by glycerolipids synthesized by LPAT2 in the cytoplasm (Kim and Huang, 2004). Our findings extend this suggestion to include the flow of glycerolipids from the plastids to the cytoplasm. The *lpat2*

Figure 10. (continued).

underdeveloped seeds are indicated with an asterisk, whereas the aborted ovules cannot be seen. Magnified, autofluorescent images of 6- and 10-DAF siliques taken under a fluorescent microscope reveal three types of ovules or seeds: shrunken, unfertilized ovules (arrows), fertilized embryo whose development stopped at the globular stage (asterisks), and fertilized embryo on a normal developmental track (arrowheads).

Table 2. Seed Production from Selfing of T2 Homozygous (*lpat2*/*lpat2*) and Heterozygous (*LPAT2*/*lpat2*) Arabidopsis Plants That Had Been Transformed with *LPAT2P:LPAT2-cDNA*

Genotypes of T2 Lines	Selfing of: Wild Type	*LPAT2*/*lpat2*	*LPAT2*/*lpat2* + *LPAT2P:LPAT2*-c	*lpat2*/*lpat2* + *LPAT2P:LPAT2*-c
	Number of seeds/silique (percentage of the wild type)			
		Seed:aborted ovules[a]		
1	51 (100%)	27 + 22 (53%) (50:50) $P < 0.05$	48 (92%)	41 (79%)
2	52 (100%)	22 + 28 (42%) (50:50) $P < 0.05$	44 (85%)	48 (92%)
3	51 (100%)	22 + 27 (43%) (50:50) $P < 0.05$	37 (71%)	42 (81%)
4	52 (100%)	26 + 29 (42%) (50:50) $P < 0.05$	45 (87%)	44 (85%)
5	53 (100%)	22 + 27 (42%) (50:50) $P < 0.05$	36 (69%)	–
Average	52 (100%)	23 + 27 (46%) (50:50) $P < 0.05$	42 (81%)	44 (85%)

The numbers of seeds or aborted ovules were the average per silique from five siliques (and proportional to the wild type).
[a] Only the *LPAT2*/*lpat2* offspring were examined for number of aborted ovules because the examination was time consuming.

female gametophyte cannot obtain glycerolipids synthesized in the plastid LPAT1 for survival. Nevertheless, our suggestion does not exclude some exchanges of glycerolipids between the two systems, and massive flow of acyl ingredients from the plastids to the cytoplasm for desaturation has been well documented (Ohlrogge and Browse, 1995).

Whereas the plastid-synthesized glycerolipids form the photosynthetic membranes, the cytoplasm-synthesized glycerolipids have more diverse functions. They can be phospholipids in all cytoplasmic membranes as structural components, TAGs in seeds as stored food for germination, TAGs in fruit as attractants to animals resulting in seed dispersion, and lipid signal molecules (Ohlrogge and Browse, 1995). In Arabidopsis, the lone ER-located AtLPAT2 acts at a metabolic pivotal point, whose product PA is converted to diverse glycerolipids. These glycerolipids, such as the lipid signal molecules, are synthesized by arrays of enzymes encoded by many genes (Wang, 2001). The LPAT gene system is unlike most other gene systems in Arabidopsis, which usually include many copies of similar genes to conduct redundant or specialized functions (Bouche and Bouchez, 2001). Nevertheless, the cytoplasmic LPAT system has specialized to include an LPAT3 to presumably handle the massive membrane turnover in the pollen tube. It is unknown whether pollen-specific LPATs are present in other species. Some other species possess seed-specific LPATs to catalyze acylation of the *sn*-2 position of seed storage TAGs with uncommon acyl groups, such as C-12 in coconut (Oo and Huang, 1989; Knutzon et al., 1995) and C-22:1 in meadowfoam (Laurant and Huang, 1992; Hanke et al., 1995). Although the uncommon C-22:1 (erucic) moiety occurs in Arabidopsis seed TAGs, it is restricted to the *sn*-1 and -3 positions, whose acylation is catalyzed by GPAT and diacylglycerol AT, respectively, and Arabidopsis does not have a seed-specific LPAT.

The functions of LPAT4 and 5 remain unknown. LPAT4 and 5 are similar in having low but ubiquitous expression and the four conserved domains found in many other acyltransferases.

Table 3. Seed Production from Selfing Arabidopsis *LPAT2*/*lpat2* + *LPAT2*P:*LPAT3* cDNA Plants

Plant (T3) *LPAT2*/*lpat2*+ *LPAT2*P:*LPAT3*-c	Normal Seeds (Normal Embryo)	Abnormal Seeds (Aborted Embryo)	Desiccated Remnant (Aborted Ovules)	Total
1	32 (62%)	17 (33%)	3 (5%)	52 (100%)
2	25 (52%)	18 (38%)	5 (10%)	48 (100%)
3	20 (43%)	15 (31%)	12 (26%)	47 (100%)
4	26 (54%)	17 (35%)	5 (11%)	48 (100%)
5	30 (60%)	16 (32%)	4 (8%)	50 (100%)
Average	27 (54%)	17 (34%)	6 (12%)	50 (100%)

Three types of seeds/ovules were identified in the siliques: normal seeds containing full-size embryos, abnormal seeds containing aborted embryos, and aborted white ovules. Each number represents the average seed or desiccated remnant from five siliques (and proportion in the siliques).

Lysates of transformed yeast containing LPAT4 and 5 had LPAT enzyme activity in our in vitro assay system not higher than that in the control yeast lysate containing no LPAT4 and 5. Whether they catalyze the acylation of LPA other than LPA-18:1 or other lipids from acyl-CoA remains to be seen, and thus terming them LPAT4 and 5 in this report is tentative.

METHODS

Plant Materials and Growth Conditions

Seeds potentially containing a T-DNA inserted in the At3g57650 locus (*LPAT*2, Salk_058130) were obtained from the Salk Institute (http://signal.salk.eud/cgi-bin/tdnaexpress) via the Arabidopsis Biological Resource Center (Ohio State University, Columbus). These seeds and seeds of the wild type (ecotype Columbia), as well as various transgenic plants, were grown to flowering in a growth chamber maintained at 100 μE m^{-2} s^{-1} and 20°C under a 16-h-light/8-h-dark photoperiod.

For the studies of *LPAT* transcripts by RT-PCR, the following organs were collected: siliques of mixed development stages, unopened flowers, rosette leaves, and stems were obtained from mature plants; roots were collected from seedlings grown for 10 d on MS medium (Gibco, Grand Island, NY); developing embryos were dissected from seeds in siliques 10 (termed early maturation) and 18 (late maturation) DAF; and 2-d-old seedlings were obtained from seeds grown on MS medium. Mature pollens were harvested by the following procedure: 100 just-opened flowers were suspended in water in a tube, and the tube was vortexed. The released pollen suspended in water was collected on a Nitex filter (Tetko, Elmsford, NY) with 20 × 20-μm openings.

Seeds of the wild type and three lines of *LPAT*2/*lpat*2 + *LPAT*2P:*LPAT*3-c were grown for 10 d on agar plates containing MS medium. The plantlets were divided into shoots and roots for the analyses of the presence of *LPAT*2-3 transcripts.

Subcellular Fractionation of the Sporophytic Anther Extract

Brassica rapa anthers were chopped in 0.1 M Hepes-NaOH, pH 7.5, and 0.4 M sucrose with a razor blade and ground gently with a mortar and pestle. The homogenate was filtered through a Nitex cloth (20 × 20-μm pore size), which retained most of the microspores (~25-μm diameter) and the unlysed outer anther cells that were more difficult to be broken than the cell wall–depleted tapetum cells. The filtrate was regarded as the crude extract, which represented materials mostly from the tapetum cells. It was centrifuged successively at 1000*g* for 10 min, 10,000*g* for 30 min, and 100,000*g* for 90 min to produce the 1-k*g*, 10-k*g*, and 100-k*g* pellets (resuspended in the same grinding buffer) and a 100-kg supernatant. The subfractions were subjected to SDS-PAGE and immunoblotting analyses.

DNA Database Search and Sequence Analyses

One plastid (LPAT1) and four putative cytoplasm (LPAT2-5) LPATs of *Arabidopsis thaliana* and related LPATs from other sources were identified from The Arabidopsis Information Resource (http://www.Arabidopsis.org) and GenBank via amino acid sequence similarities with use of a maize (*Zea mays*) LPAT (Z29518) and a Brassica LPAT (AF111161) as queries (Kim and Huang, 2004).

Protein sequence alignments among the four Arabidopsis putative cytoplasmic LPATs were conducted by the ClustalW algorithm (Thompson et al., 1994) with use of the residue substitution matrix (blosum62mt2) of the AlignX application of Vector NTI Suite (InforMax, North Bethesda, MD). A phylogenetic tree of the aligned sequences was built with use of the neighbor-joining method (Saitou and Nei, 1987).

The Arabidopsis MPSS database (http://mpss.udel.edu/at/java.html) was used to estimate the prevalence of transcripts of *LPAT*1-4 in cDNA libraries of five organs. The signatures of 17-mer tags generated via cutting the transcript cDNA in the libraries at the *Sau*3A restriction site were normalized to transcripts per million to facilitate comparisons among libraries. The transcripts per million were based on 1,963,474; 1,791,360; 2,885,229; 3,645,414; and 2,018,785 signatures in callus, inflorescence, leaf, root, and silique libraries, respectively.

RT-PCR and cDNA Cloning of *LPAT* Genes

RT-PCR analyses were performed with gene-specific primers for *LPAT*2-5 as described (Kim and Huang, 2004). Gene-specific primers were designed to correspond to the sequence diversity regions between the 3′ terminal coding region and the 3′ untranslated region. The respective forward and reverse primers for *LPAT*2-5 were 5′-GCGTACTAACTCTTGGAGCAA-3′ and 5′-CAAAACTGACACGCGCTTCTT-3′ for a 294-bp fragment, 5′-TTTCCTTGTATTCGGTGGTTTC-3′ and 5′-TGGTTGCAATTGTTAGACAACA-3′ for a 341-bp fragment, 5′-GAAACAACAACAGGTCACTAAAC-3′and 5′-TTACAATTCTACATGAGCTTGTA-3′ for a 461-bp fragment, and 5′-GATTGCCTTCACCACCATCTG-3′ and 5′-CCCAAGCTATGATCTAACATGTG-3′ for a 325-bp fragment.

Full-length cDNAs of *LPAT*2-3 were amplified by RT-PCR from RNA of flowers and cloned into a pGEM-T vector. The primers represented sequences at the 5′ terminal end of the ORF and the untranslated region. For *LPAT*2-3, the primers were (p1) 5′-TTGAGGATGGTGATTGCTGCA-3′ and (p2) 5′-GTTTTTACTTCTCCTTCTCCG-3′, and 5′-TCAGACATGAAGATCCCTGCG-3′ and (p5) 5′-GTCCTAAGCAGAAATAAGCTG-3′.

The primers, p1, p2, p5, (p3) 5′-ACTGAAACGTGGAAATACCAGTACATCCATA-3′, and (p4) 5′-ATTGCATAGTTCAAAACTTCAAAGTTGGCCA-3′ were used for genotyping *LPAT*2-3 and *lpat*2 in the wild type, mutants, and their transgenic plants. The uses of these primers are shown in Figure 10A.

DNA-PCR was performed to evaluate whether the above RT-PCR was performed at conditions that would reveal the quantities of the *LPAT* transcripts. It was performed with the same gene-specific primers used for the RT-PCR and LPAT cDNA from the respective clones as templates as well as the same PCR cycle numbers.

LPAT Promoter:*GUS* Construction and Histochemical Localization of *GUS* Expression

The promoter regions of *LPAT*2-5 were each chosen from the sequence 5′ upstream of the predicted translation initiation site and the adjacent 5′ upstream gene. They were amplified by PCR with specific primers and leaf DNA as a template and then inserted into a pMOSBlue vector (Amersham Pharmacia Biotech, Piscataway, NJ) to produce unique recognition sites by restriction endonucleases. The specific primers for *LPAT*2-5 were 5′-GAGGATAAAATGCCAAAGATTGAATGA-3′ and 5′-CCTCAAAAAATCCCACCAACAAAAG-3′, 5′-TCTACGAGGCCAACGGAAGATCCCT-3′ and 5′-GTCTGAGAGAGATAAGGAACAACAC-3′, 5′-TGCTCCGCTTCTACGGAACCACTTC-3′ and 5′-TTCCAGATAAACCTCAAGACAAAACTGC-3′, and 5′-GACTGAGAAGGAGAAGCAGCAGATT-3′ and 5′-ACACCTTAAGATAATCTAATTAACCTCCC-3′, respectively. Each of the inserts was confirmed by DNA sequencing.

For each of *LPAT*2-5, an *LPAT* promoter:*GUS* was constructed by inserting the above-mentioned promoter sequence, cut from pMOS*Blue*-LPAT, into pBI101 in frame with *GUS*. The products of *LPAT*2P:*GUS*, *LPAT*3P:*GUS*, *LPAT*4P:*GUS*, and *LPAT*5P:*GUS* had a 3.0-kb *Xba*I-*Sma*I fragment, a 2.0-kb *Hin*dIII-*Sma*I fragment, a 1.8-kb *Hin*dIII-*Sma*I fragment, and a 0.9-kb *Xba*I-*Sma*I fragment, respectively, representing the promoters. T1 or T2 plants showing kanamycin resistance were investigated for *GUS* expression patterns.

GUS staining of organs was performed with use of the substrate 5-bromo-4-chloro-3-indolyl β-D-glucuronide according to the method described by Jefferson (1987). Potassium ferricyanide and ferrocyanide (3 mM) were added to limit diffusion of GUS reaction products. Samples were incubated in a β-D-glucuronide solution at 37°C for 20 h. After incubation, samples were cleared in ethanol and photographed.

DNA and RNA Hybridization of Leaf Samples from Plants of Various Genotypes

DNA from plants of various genotypes was isolated from leaves with use of a CTAB procedure described by Dellaporta et al. (1983) and digested with *Pst*I. One *Pst*I site is at the opposite ends of *LPAT*2 and 1 is in the T-DNA. The inserted T-DNA, *LPAT*2, and *lpat*2 were detected by hybridization of genomic DNA with a ^{32}P-labeled DNA probe. The probe was obtained from DNA of the heterozygous mutant with use of primers p1 and LBa1 and labeled with ^{32}P-dCTP with use of the Multiprimer DNA labeling kit (Amersham Phamacia Biotech). The probe was ~1.6 kb and contained 1.2 kb of the 5′ terminal portion of the *LPAT*2 coding region and 0.4 kb of the 5′ terminal portion of the T-DNA. The procedure for hybridization was as described previously (Kim et al., 2001).

Total RNAs were isolated from leaves as described (Verwoerd et al., 1989). RNA hybridization probe and the procedure were as described for DNA hybridization.

Expression of *LPAT*s in *Escherichia coli* JC201 and Assay for in Vitro LPAT Enzyme Activities

Full-length fragments of cDNAs of *LPAT*2-5 were amplified by RT-PCR from RNA of flowers. Unique restriction sites were generated by PCR: *Bam*HI-*Hin*dIII with primers 5′-GGATCCGATGGTGATTGCTGCAGCT-GTC-3′ and 5′-AAGCTTTTACTTCTCCTTCTCCGTTTC-3′ for *LPAT*2; *Bam*HI-*Sal*I with 5′-GGATCCCATGAAGATCCCTGCGGCTCTT-3′ and 5′-GTCGACCTAAGCAGAAATAAGCTGTTC-3′ for *LPAT*3; *Sph*I-*Hin*dIII with primers 5′-GCATGCGATGGAAGTTTGCGGGGATCTG-3′ and 5′-AAGCTTTTAATGGTTTTTAACTTTACAAGAATC-3′ for *LPAT*4; and *Sph*I-*Hin*dIII with primers 5′-GCATGCAATGGAAAAAAAGAGTGTACCA-3′ and 5′-AAGCTTTTATTTGTTTACTAATTTGAGGGAATT-3′ for *LPAT*5. The fragments were ligated in frame into the pQE31 expression vector. The constructs were transformed into the *E. coli* strain, JC201, which had been previously transformed with pREP4 (Qiagen, Valencia, CA) that confers kanamycin resistance and expresses the *lac* repressor protein LacI. The bacteria were grown on Luria-Bertani agar at 30°C and 42°C. Successful functional complement would be achieved if the transformed bacteria grew at 42°C after IPTG induction.

The following procedure was used to prepare bacteria extracts for LPAT enzyme assay. A 1-mL overnight culture in a Luria-Bertani liquid medium was used to inoculate a 200-mL medium containing 100 μg/mL of streptomycin, 50 μg/mL of ampicillin, and 25 μg/mL of kanamycin. The culture was allowed to grow at 30°C until the A_{600} reached ~0.5. IPTG was added to a final concentration of 0.2 mM, and induction was allowed to continue for 1 h. The culture did not grow well beyond this 1-h period, which indicates the lethality of LPAT2-5 in the bacteria cells. After the 1-h induction, the cells were pelleted by low-speed centrifugation, and the pellet was resuspended in 4 mL of 50 mM Tris-HCl, pH 8.0, 2 mM $MgCl_2$, and 2 mM DTT. The resuspended cells were disrupted by sonication with a 40T probe in a Braun-Sonic 2000 ultrasonic generator (Freeport, IL) with a digital meter reading of 200. The total extract was centrifuged at 10,000*g* for 15 min at 4°C to remove unbroken bacteria and debris. The supernatant was centrifuged at 100,000*g* for 1.5 h at 4°C. The pellet containing membranes was resuspended in 1 mL of the above buffer and stored at −80°C. It was used to assay for LPAT activity with LPA-18:1 and ^{14}C-CoA-18:1 or CoA-16:0 as described previously (Kim and Huang, 2004) and for SDS-PAGE and immunoblotting analyses.

Expression of *LPAT*s in *Saccharomyces cerevisiae* and Assay for in Vitro LPAT Enzyme Activities

Full-length ORF fragments of cDNAs of *LPAT*2-5 were reamplified by PCR from LPAT cDNA clones with the following primers: 5′-GCGATGGT-GATTGCTGCAGCTGTC-3′ and 5′-CTTTTACTTCTCCTTCTCCGTTTC-3′ for *LPAT*2, 5′-GCCATGAAGATCCCTGCGGCTCTT-3′ and 5′-GACCT-AAGCAGAAATAAGCTGTTC-3′ for *LPAT*3, 5′-GCGATGGAAGTTTGC-GGGGATCTG-3′ and 5′-CTTTTAATGGTTTTTAACTTTACAAGA-3′ for *LPAT*4, and 5′-GCAATGGAAAAAAAGAGTGTACCA-3′ and 5′-CTTTT-ATTTGTTTACTAATTTGAGGGA-3′ for *LPAT*5.

The cDNAs were cloned into pYES2.1 TOPO TA cloning vector with use of topoisomerase (Invitrogen, Carlsbad, CA) to produce pYES-LPAT2-5. The plasmids with the *LPAT* inserts were first transformed into competent *E. coli*, TOP10F′. Plasmid DNAs from the resulting bacterial colonies were isolated and confirmed of their inserted *LPAT* sequences by sequencing with use of the GAL1 forward primer (5′-AATATACCTCTATA-CTTTAACGTC-3′) and V5 C-term reverse DNA sequencing primer (5′-ACCGAGGAGAGGGTTAGGGAT-3′). Then, the plasmids containing *LPAT*s were transformed into *S. cerevisiae*, strain INVSc1, and the transformed cells were selected on plates containing the SC-U minimal medium (0.67% yeast nitrogen base, 2% glucose, complete supplement mixture lacking uracil, and 20 g/L agar).

DNA was extracted from the transformed yeast with use of a method described by M. Kaeberlein (http://web.mit.edu/guarente/protocols/quickprep.html), and the presence of *LPAT*s of the expected sequences was confirmed by obtaining PCR fragments with use of the above-mentioned gene-specific primers. Each transformed yeast was grown to the late-log phase in the SC-U medium containing 2% glucose. The cells were harvested by centrifugation and inoculated at a concentration of $OD_{600} = 0.4$ in an induction medium (SC-U medium containing 2% galactose). The induction was allowed to proceed for 4 h. The galactose would induce high-level expression of the transgene controlled by the *GAL*1 promoter in the plasmid vector.

The yeast cells were harvested by centrifugation, washed once with water, and harvested again. The washed cells were resuspended in 50 mM Na phosphate, pH 7.4, 1 mM EDTA, 5% glycerol, and 1 mM PMSF and broken with glass beads and a mortar and pestle. The samples were centrifuged at 8000*g* for 15 min at 4°C to remove cell debris. The resulting supernatant was the lysate, which was used for protein analyses by SDS-PAGE and LPAT activity assays (preceding section). The lysate was also centrifuged at 100,000*g* for 90 min to yield a membrane pellet for use in immunoblotting.

Preparation of Antibodies against LPAT2 and SDS-PAGE and Immunoblotting

Among the four putative LPAT2-5, LPAT2 has a unique peptide, KPKDNHHPESSSQTETEKEK, at the C terminus (Figure 2). All other Arabidopsis proteins do not have a sequence similar to this unique peptide. The Brassica LPAT2 related to Arabidopsis LPAT2 has a similar sequence, KPKDNHQSGPSSQTEVEEK, at its C terminus. A synthetic peptide corresponding to the Arabidopsis LPAT2 peptide was made, and rabbit antibodies against it were prepared via a procedure described earlier (Wang et al., 1997). Antibodies against castor bean calreticulin were kindly provided by Sean Coughlan and Tony Kinney.

SDS-PAGE and immunoblotting of the gel were performed by procedures described earlier (Kim and Huang, 2004). Protein quantities in the bacterial and yeast extracts were determined with the Bradford method (Bradford, 1976) and BSA as the standard.

Immunofluorescence Microscopy

Parafilm sections 7 μm thick of Arabidopsis flower buds and *B. rapa* anthers were used. Double immunolabeling with two polyclonal antibodies was performed as previously described, with modifications (Li et al., 2002). Primary antibodies included rabbit anticalreticulin (1:1000) against the protein from castor bean, chicken anti-PAP (1:500; Brassica plastid lipid-associated protein) (Kim et al., 2001), and rabbit anti-LPAT2 (1:50). Organ sections on slides were incubated with the primary antibodies (anticalreticulin) at 4°C overnight. After the antibody solution was removed, the sections were washed with PBST (0.05% Tween 20 in PBS) three times for 5 min each. The sections were incubated with Cy3-conjugated Fab fragment goat anti-rabbit IgG (H+L) (1:50 dilution) at room temperature for 3 to 5 h in the dark. The sections were rinsed briefly and post-fixed with 4% paraformaldehyde in 50 mM Na-phosphate buffer, pH 7.4, at room temperature for 20 min. After being washed with PBST three times for 5 min each, the sections were incubated with primary antibodies (rabbit anti-LPAT2 or chicken anti-PAP) at 4°C overnight in the dark and then Cy5-conjugated goat anti-rabbit IgG (H+L) (1:200 dilution) at room temperature for 1 h. A drop of antifade solution (Molecular Probes, Eugene, OR) was added to the section, which was then covered with a cover slip and sealed with nail polish. All confocal images were collected with the use of a Leica TCS SP2 confocal microscopy system (Leica Microsystems, Wetzlar, Germany), and three-dimensional images were created with the combination of multiple serial optical sections. Images were processed with the use of Adobe Photoshop software (San Jose, CA).

Construction of *LPAT*2P:*LPAT*2-cDNA and *LPAT*2P:*LPAT*3-cDNA and Their Transformation into a Heterozygous (*LPAT*2/*lpat*2) Mutant

*LPAT*2P:*LPAT*2-c and *LPAT*2P:*LPAT*3-c, containing 3.0 kb of the *LPAT*2 promoter and the full-length cDNA of *LPAT*2 and *LPAT*3, respectively, were constructed. *GUS* in pBI101 harboring *LPAT*2P:*GUS* was replaced with either *LPAT*2-c or *LPAT*3-c, which were obtained from pGEM-T containing these cDNA. pBI101 harboring *LPAT*2P:*LPAT*2-c or *LPAT*2P:*LPAT*3-c was transformed into heterozygous (*LPAT*2/*lpat*2) mutants by the floral dip method with use of the *Agrobacterium tumefaciens* strain GV3101. Selection for kanamycin resistance was made via *npt*II in pBI101 because the T-DNA in the *LPAT*2/*lpat*2 heterozygous mutant did not confer kanamycin resistance. Kanamycin-resistant seedlings (T1) on a Petri dish were transferred to soil. The T2 and T3 generation plants were examined for *lpat*2, *LPAT*2, and *LPAT*3 by PCR and for seed appearance by stereomicroscopy (LEICAMZ125; Leica Microsystems).

Phenotypes and Genetic Analyses of *LPAT*2/*lpat*2 Mutants and Transgenic Plants

Thirteen seeds potentially containing *lpat*2 (a T-DNA inserted into *LPAT*2) were obtained from the Salk Institute. They were grown to mature plants, and leaves were analyzed for *LPAT*2 and *lpat*2 by PCR. No *lpat*2/*lpat*2 individual was found. Five *LPAT*2/*lpat*2 heterozygous individuals identified all had vegetative parts quite similar to those of wild types, with a minor exception that their leaves were slightly elongated. They all produced siliques, each of which was half filled with seeds and half with aborted ovules or embryos. The progeny of each of these five heterozygous individuals were kanamycin sensitive, even though the T-DNA inserted into *LPAT*2 was supposed to contain *npt*II. One of the five heterozygous individuals was found to contain only one copy of T-DNA per diploid genome, as revealed by DNA hybridization analysis. From this individual, a 1.6-kb DNA fragment was generated by PCR with p1 and LBa1 primers and sequenced. The sequence confirmed that *LPAT*2 was inserted by a T-DNA in the fifth intron after nucleotide 21,362,009 in chromosome 3 (Figure 2). This individual was used for all subsequent studies.

The embryo sacs of the wild type and the heterozygous mutant were observed by microscopy. The pistils of different developmental stages were cut into 1-mm segments and fixed, dehydrated, infiltrated, and embedded in Embed 812 (Electron Microscopy Sciences, Hatfield, PA) as described previously (Christensen et al., 1997). Thin sections (10 μm) were stained with tuluidine blue for light microscopy with a Nikon MICROPHOT-FXA (Tokyo, Japan) attached to a Spot digital camera or lead citrate and uranyl acetate for electron microscopy (Platt et al., 1998).

Lipid Analysis

Rosette leaves were immediately frozen in liquid nitrogen after being harvested, and the lipids were extracted according to the protocol of the Lipodomics Center at Kansas State University (http://www.ksu.edu/lipid/lipidomics/leaf-extraction.html). The acyl moieties of the lipids were saponified with alkaline in ethanol, and the acidified samples of free fatty acids were derivatized to methyl esters with boron trifluoride in methanol, which were subjected to gas–liquid chromatography analysis.

ACKNOWLEDGMENTS

The research was supported by the National Science Foundation Grant MCB-0131358 and the USDA (National Research Initiative Competitive Grant 2000-01512). We sincerely thank Jack Coleman for the *E. coli* JC201 strain, Joseph Ecker of the Salk Institute (La Jolla, CA) and the Arabidopsis Biological Resource Center (Ohio State University, Columbus) for the T-DNA–inserted *LPAT*2 Arabidopsis mutant, Sean Coughlan and Tony Kinney (DuPont, Wilmington, DE) for the antibodies against castor bean calreticulin, Kai Hsieh for advice on immunofluorescence microscopy, and the Lipidomics Center (Kansas State University, Manhattan) for lipid analysis.

Received December 19, 2004; accepted February 2, 2005.

REFERENCES

Becker, J.D., Boavida, L.C., Carneiro, J., Haury, M., and Feijo, J.A. (2003). Transcriptional profiling of Arabidopsis tissues reveals the unique characteristics of the pollen transcriptome. Plant Physiol. **133,** 713–725.

Bouche, N., and Bouchez, D. (2001). Arabidopsis gene knockout: Phenotypes wanted. Curr. Opin. Plant Biol. **4,** 111–117.

Bourgis, F., Kader, J.C., Barret, P., Renard, M., Robinson, D., Robinson, C., Delseny, M., and Roscoe, T.J. (1999). A plastidal lysophosphatidic acid acyltransferase from oilseed rape. Plant Physiol. **120,** 913–921.

Bradford, M.M. (1976). A rapid and sensitive method for the quantitation of microgram quantities of protein utilizing the principle of protein-dye-binding. Anal. Biochem. **72,** 248–254.

Brown, A.P., Brough, C.L., Kroon, J.T.M., and Slabas, A.R. (1995). Identification of a cDNA that encodes a 1-acyl-*sn*-glycerol-3-phosphate acyltransferase from *Limnanthes douglasii*. Plant Mol. Biol. **29,** 267–278.

Brown, A.P., Coleman, J., Tommey, A.M., Watson, M.D., and Slabas, A.R. (1994). Isolation and characterization of a maize cDNA that complements a 1-acyl-*sn*-glycerol-3-phosphate acyltaransferase mutant of *Escherichia coli* and encodes a protein which similarities to other acyltransferases. Plant Mol. Biol. **26,** 211–223.

Bursten, S.L., Harris, W.E., Bomsztyk, K., and Lovett, D. (1991). Interleukin-1 rapidly stimulates lysophosphatidate acyltransferase and

phosphatidate phosphohydrolase activities in human mesangial cells. J. Biol. Chem. **266,** 20732–20743.

Cao, Y.Z., Oo, K.C., and Huang, A.H.C. (1990). Lysophosphatidate acyltransferase in the microsomes from maturing seeds of meadowfoam (*Limnanthes alba*). Plant Physiol. **94,** 1199–1206.

Christensen, C.A., King, E.J., Jordan, J.R., and Drews, G.N. (1997). Megagametogenesis in Arabidopsis wild type and *Gf* mutant. Sex. Plant Reprod. **10,** 49–64.

Coleman, J. (1990). Characterization of *Escherichia coli* cells deficient in 1-acyl-*sn*-glycerol-3-phosphate acyltransferase activity. J. Biol. Chem. **265,** 17215–17221.

Costa, L.M., Gutierrez-Marcos, J.F., and Dickinson, H.G. (2004). More than a yolk: The short life and complex times of the plant endosperm. Trends Plant Sci. **9,** 507–514.

Dellaporta, S.L., Wood, J., and Hicks, J.B. (1983). A plant DNA minipreparation: Version II. Plant Mol. Biol. Rep. **1,** 19.

Drews, G.N., and Yadegari, R. (2002). Development and function of the angiosperm female gametophyte. Annu. Rev. Genet. **36,** 99–124.

Frentzen, M. (1998). Acyltransferases from basic science to modified seed oils. Fett/Lipid **100,** 161–166.

Giniger, E., Branum, S.M., and Patashne, M. (1985). Specific DNA binding of GAL4, a positive regulatory protein of yeast. Cell **40,** 767–774.

Hanke, C., Wolter, F.P., Coleman, J., Peterek, G., and Frentzen, M. (1995). A plant acyltransferase involved in triacylglycerols biosynthesis complements an *Escherichia coli sn*-1-acylglycerol-3-phosphate acyltransferase mutant. Eur. J. Biochem. **232,** 806–810.

Honys, D., and Twell, D. (2003). Comparative analysis of the Arabidopsis pollen transcriptome. Plant Physiol. **132,** 640–652.

Ishizaki, O., Nishida, I., Agata, K., Eguchi, G., and Murata, N. (1988). Cloning and nucleotide sequence of cDNA for the plastid glycerol-3-phosphate acyltransferase from squash. FEBS Lett. **238,** 424–430.

Jefferson, R.A. (1987). Assaying chimeric genes in plants: The *GUS* gene fusion system. Plant Mol. Biol. Rep. **5,** 387–405.

Kim, H.U., and Huang, A.H.C. (2004). Plastid lysophosphatidyl acyltransferase is essential for embryo development in Arabidopsis. Plant Physiol. **134,** 1206–1216.

Kim, H.U., Wu, S.S.H., Ratnayake, C., and Huang, A.H.C. (2001). *Brassica rapa* has three genes that encode proteins associated with different neutral lipids in plastids of specific tissues. Plant Physiol. **126,** 330–341.

Knutzon, D.S., Lardizabal, K.D., Nelsen, J.S., Bleibaum, J.L., Davies, H.M., and Metz, J.C. (1995). Cloning of a coconut endosperm cDNA encoding a 1-acyl-*sn*-glycerol-3-phosphate acyltransferase that accepts medium-chain-length substrates. Plant Physiol. **109,** 999–1006.

Kunst, L.J., Browse, J., and Somerville, C. (1988). Altered regulation of lipid biosynthesis in a mutant of Arabidopsis deficient in chloroplast glycerol-3-phosphate acyltransferase activity. Proc. Natl. Acad. Sci. USA **85,** 4143–4147.

Laage, R., and Langosch, D. (2001). Strategies for prokaryotic expression of eukaryotic membrane proteins. Traffic **2,** 99–104.

Laurant, P., and Huang, A.H.C. (1992). Organ and development specific acyl CoA lysophosphatidate acyltransferase in palm and meadowfoam. Plant Physiol. **99,** 1711–1715.

Li, Y., Rogers, S.W., Tse, Y.C., Lo, S.W., Sun, S.S.M., Jauh, G., and Jiang, L. (2002). BP-80 and homologs are concentrated on post-Golgi, probable lytic prevacuolar compartments. Plant Cell Physiol. **43,** 726–742.

Mascarenhas, J.P. (1993). Molecular mechanisms of pollen tube growth and differentiation. Plant Cell **5,** 1303–1314.

Meyers, B.C., Lee, D.K., Vu, T.H., Tej, S.S., Edberg, S.B., Matvienko, M., and Tindell, L.D. (2004). Arabidopsis MPSS. An online resource for quantitative expression analysis. Plant Physiol. **135,** 801–813.

Murata, N., and Tasaka, Y. (1997). Glycerol-3-phosphate acyltransferase in plants. Biochim. Biophys. Acta **1348,** 10–16.

Ohlrogge, J., and Browse, J. (1995). Lipid biosynthesis. Plant Cell **7,** 957–970.

Oo, K.C., and Huang, A.H.C. (1989). Lysophosphatidyl acyltransferase activities in the microsomes from palm endosperm, maize scutellum, and rapeseed cotyledon of maturing seeds. Plant Physiol. **91,** 1288–1295.

Papp, S., Dziak, E., Michalak, M., and Opas, M. (2003). Is all the endoplasmic reticulum created equal? The effects of the heterogeneous distribution of endoplasmic reticulum Ca2+-handling proteins. J. Cell Biol. **160,** 475–479.

Platt, K.A., Huang, A.H.C., and Thomson, W.W. (1998). Ultrastructural study of lipid accumulation in tapetal cells of *Brassica napus* L. cv. *Westar* during microsporogenesis. Int. J. Plant Sci. **159,** 724–737.

Saitou, N., and Nei, M. (1987). The neighbor-joining method: A new method for reconstructing phylogenetic trees. Mol. Biol. Evol. **4,** 406–425.

Somerville, C., Browse, J., Jaworski, J.G., and Ohlrogge, J.B. (2000). Lipids. In Biochemistry and Molecular Biology of Plants, B.B. Buchanan, W. Gruissem, and R.L. Jones, eds (Rockville, MD: American Society of Plant Physiologists), pp. 456–527.

Thompson, J.D., Higgins, D.G., and Gibson, T.J. (1994). CLUSTAL W: Improving the sensitivity of progressive multiple sequence alignment through sequence weighting, position-specific gap penalties and weight matrix choice. Nucleic Acids Res. **22,** 4673–4680.

Verwoerd, T.C., Dekker, B.M.M., and Hoekema, A. (1989). A small scale procedure for the rapid isolation of plant RNAs. Nucleic Acids Res. **17,** 2362.

Voelker, T., and Kinney, A.J. (2001). Variations in the biosynthesis of seed storage lipids. Annu. Rev. Plant Physiol. Plant Mol. Biol. **52,** 335–361.

Wang, T.W., Balsamo, R.A., Ratnayake, C., Platt, K.A., Ting, J.T.L., and Huang, A.H.C. (1997). Identification, subcellular localization, and developmental studies of oleosins in the anthers of *Brassica napus*. Plant J. **11,** 475–487.

Wang, X. (2001). Plant phospholipases. Annu. Rev. Plant Physiol. Plant Mol. Biol. **52,** 211–231.

Yu, B., Wakao, S., Fan, J., and Benning, C. (2004). Loss of plastic lysophosphatidic acid acyltransferase cause embryo-lethality in Arabidopsis. Plant Cell Physiol. **45,** 503–510.

Zborowski, J., and Wojtczak, L. (1969). Phospholipid synthesis in rat liver mitochondria. Biochim. Biophys. Acta **187,** 73–84.

Zheng, Z., Xia, Q., Dauk, M., Shen, W., Selvaraj, G., and Zou, J. (2003). Arabidopsis *AtGPAT*1, a member of membrane-bound glycerol-3-phosphate acyltransferase gene family, is essential for tapetum differentiation and male fertility. Plant Cell **15,** 1872–1887.